

# Politecnico di Milano

---

SCHOOL OF INDUSTRIAL AND INFORMATION ENGINEERING

Master of Science – Aerospace Engineering



## Thesis Title

Supervisor

**Title Name SURMANE**

Co-Supervisor

**Title Name SURNAME**

Candidate

**Claudio CACCIA – 820091**

---

**Academic Year 2019 – 2020**



# Acknowledgements

Thanks



# Abstract

This thesis describes bla bla...

***Keywords***— one, two, three, four



# Sommario

In questa tesi bla bla...





# Contents

<b>Acknowledgements</b>	<b>iii</b>
<b>Abstract</b>	<b>v</b>
<b>Sommario</b>	<b>vii</b>
<b>Contents</b>	<b>x</b>
<b>List of Figures</b>	<b>xi</b>
<b>List of Tables</b>	<b>xiii</b>
<b>1 Introduction</b>	<b>1</b>
<b>2 Physical aspects of Fluid-Structure Interaction problems</b>	<b>3</b>
2.1 Description of motion . . . . .	3
2.1.1 Eulerian perspective . . . . .	3
2.1.2 Lagrangian perspective . . . . .	4
2.1.3 ALE method . . . . .	5
2.2 Domains and interface . . . . .	6
2.2.1 Fluid domain . . . . .	6
2.2.2 Solid domain . . . . .	7
2.2.3 Models with reduced dimensionality: beams . . . . .	8
2.2.4 Interface and interaction . . . . .	9
2.3 Classification of FSI problems . . . . .	10
2.3.1 Dimensional analysis . . . . .	10
2.3.2 Dimensional analysis in fluid domain . . . . .	11
2.3.3 Dimensional analysis in solid domain . . . . .	12
2.3.4 Dimensional analysis of coupled problems . . . . .	12
<b>3 Computational aspects of Fluid-Structure Interaction problems</b>	<b>15</b>
3.1 Monolithic and Partitioned Approach . . . . .	15
3.2 Coupling Strategies . . . . .	17
3.2.1 Explicit coupling schemes . . . . .	17
3.2.2 Implicit coupling schemes . . . . .	18
3.3 Strong coupling algorithms . . . . .	20
3.3.1 under-relaxation . . . . .	20
3.3.2 Quasi Newton Least Squares schemes . . . . .	21
3.3.3 Convergence criteria . . . . .	22
3.4 Interface Mesh and Data Mapping . . . . .	23
3.4.1 Non-conforming Mesh methods . . . . .	23

3.4.2	Conforming Mesh methods . . . . .	24
3.4.3	Data Mapping . . . . .	24
3.5	Stability: Added Mass Effect . . . . .	26
3.5.1	AME in compressible regime . . . . .	26
3.5.2	AME in incompressible regime . . . . .	26
<b>4</b>	<b>Software Packages used in this work</b>	<b>29</b>
4.1	preCICE . . . . .	29
4.1.1	Implemented coupling strategies . . . . .	29
4.1.2	Communication strategies . . . . .	32
4.1.3	Data mapping . . . . .	33
4.1.4	Configuration . . . . .	35
4.1.5	Application Program Interface . . . . .	35
4.1.6	Official Adapters . . . . .	36
4.2	MBDyn . . . . .	36
<b>5</b>	<b>MBDyn Adapter and its integration</b>	<b>37</b>
<b>6</b>	<b>Validation Test-cases</b>	<b>39</b>
<b>7</b>	<b>Conclusions</b>	<b>41</b>
	<b>Conclusions</b>	<b>41</b>
<b>A</b>	<b>First Appendix</b>	<b>45</b>
	<b>Acronyms</b>	<b>51</b>
	<b>Bibliography</b>	<b>56</b>

# List of Figures

Figure 2.1	Eulerian perspective . . . . .	4
Figure 2.2	Lagrangian perspective . . . . .	4
Figure 2.3	ALE perspective . . . . .	5
Figure 2.4	ALE mesh . . . . .	6
Figure 2.5	beam model, taken from [1] . . . . .	9
Figure 2.6	fluid solid interface . . . . .	9
Figure 3.1	monolithic approach: $S_f, S_s$ denote the fluid and the structure solutions	16
Figure 3.2	partitioned approach: $S_f, S_s$ denote the fluid and the structure solutions, while $\sigma$ and $\vec{v}$ represent coupling data . . . . .	16
Figure 3.3	Explicit coupling schemes . . . . .	18
Figure 3.4	Implicit coupling schemes . . . . .	19
Figure 3.5	non conforming mesh example . . . . .	23
Figure 3.6	conforming mesh example . . . . .	24
Figure 3.7	Examples of mapping data between non-coincident meshes: consistent (a) and conservative (b) schemes. . . . .	25



# List of Tables

Table 2.1	fluid matrix of dimension exponents . . . . .	11
-----------	---	----



# Chapter 1

## Introduction

Fluid-Structure Interaction (**FSI**) describes the mutual interaction between a moving or deformable object and a fluid in contact with it, surrounding or internal. It is present in various forms both in nature and in man-made systems: a leaf fluttering in the wind, water flowing underground or blood pumping in an artery are typical examples of fluid-structure interaction in nature. FSI occurs in engineered systems when modeling the behavior of turbomachinery, the flight characteristics of an aircraft, or the interaction of a building with the wind, just to name a few examples.

All the aforementioned problems go under the same category of FSI, even if the nature of the interaction between the solid and fluid is different. Specifically, the intensity of the exchanged quantities and the effect in the fluid and solid domains vary among different problems.

There can be multiple ways to classify FSI problems, based on the flow physics and on the behavior of the body. Incompressible flow assumption is always made for liquid-solid interaction, while both compressible and incompressible flow assumptions are made when a gas interacts with a solid, depending on the flow properties and the kind of simulation. The main application of air-solid interaction considers the determination of aerodynamic forces on structures such as aircraft wings, which is often referred to as *aeroelasticity*. Dynamic aeroelasticity is the topic that normally investigates the interaction between aerodynamic, elastic and inertial forces. Aerodynamic *flutter* (i.e. the dynamic instability of an elastic structure in a fluid flow) is one of the severe consequences of aerodynamic forces. It is responsible for destructive effects in structures and a significant example of FSI problem.

The subject may also be classified considering the behavior of the structure interacting with the fluid: a solid can be assumed rigid or deforming because of the fluid forces. Examples where rigid body assumption may be used include internal combustion engines, turbines, ships and offshore platforms. The rigid body–fluid interaction problem is simpler to some extent, nevertheless the dynamics of rigid body motion requires a solution that reflects the fluid forces. Within the deformable body–fluid interaction, the nature of the deforming body may vary from very simple linear elastic models in small strain to highly complex nonlinear deformations of inelastic materials. Examples of deforming body–fluid interaction include aeroelasticity, biomedical applications and poroelasticity.

The interaction between fluid (incompressible or compressible) and solid (rigid or deformable) can be *strong* or *weak*, depending on how much a change in one domain influences the other. An example of weakly coupled problem is aeroelasticity at high Reynolds number, while incompressible flow often leads to strongly coupled problems. This distinction can lead to different solution strategies, as briefly described below.

Physical models aren't the only way in which FSI problems can be classified. The solution

procedure employed plays a key role in building models and algorithms to solve this kind of problems. The two main approaches are: the *monolithic approach* in which both fluid and solid are treated as one single system and the *partitioned approach* in which fluid and solid are considered as two separated systems coupled only through an interface. This latter approach is often preferred when building new solution procedures as it allows to use solvers that have been already developed, tested and optimized for a specific domain. The solvers only need to be linked to a third component, which takes care of all the interaction aspects.

The partitioned approach can be further classified considering the coupling between the fluid and solid: the solution may be carried out using a *weakly coupled approach*, in which the two solvers advance without synchronization, or a *strongly coupled approach*, in which the solution for all the physics must be synchronized at every time step. Although the weakly coupled approach is used in some aerodynamic applications, it is seldom used in other areas due to instability issues. A strongly coupled approach is generally preferred, even though this leads to more complex coupling procedures at the interface between fluid and solid.

This work describes the implementation and the validation of what is called an *adapter*, that is the "glue-code" needed to interface a solver to a coupling software library, thus adopting a *partitioned approach* to solve FSI problems. The *adapter* presented here connects the software code *MultiBody Dynamics analysis software (MBDyn)* to the multiphysics coupling library *precise Code Interaction Coupling Environment (preCICE)*.

Interfacing MBDyn with preCICE has multiple advantages: on one side it extends the capabilities of MBDyn to be used in FSI simulations by connecting it with a software library which has been already connected to widely used CFD solvers; on the other side, it allows to describe and simulate FSI problems with a suite of lumped, 1D and 2D elements (i.e. rigid bodies, *beams*, *membranes*, *shells*, etc.) decoupling the shape of the object (the interface with the fluid) from its structural properties, which can be described by different models and constitutive laws.

The thesis is structured as follows:

- Section 2 introduces the reader to FSI problems and their complexity, with particular attention to the physical description of the fluid and solid domains and the interface.
- Section 3 focuses on numerical methods, describing how to computationally deal with these kind of problems: details regarding the different coupling approaches are given here.
- Section 4 explains the features of preCICE that the adapter needs to support and gives a short introduction to MBDyn, explaining the main functionalities of interest.
- Section 5 presents the adapter developed in this work, its most important features and how to configure a FSI simulation with it.
- Section 6 describes the successful validation of the adapter, the comparison of the results with some well-known benchmarks and an example of real world application.
- Section 7 summarizes the findings and outcome of this work and gives an outlook to future work on this topic.
- Finally XX appendices give further information on...



# Chapter 2

## Physical aspects of Fluid-Structure Interaction problems

Dynamic models of solids or fluids aim at describing the evolution of an initial configuration through time. Structural mechanics and fluid dynamics use different perspectives when describing the motion of respectively a solid or a fluid particle. When dealing with FSI problems the two approaches need to be combined in order to obtain a suitable description of the two domains and their interface: this aspect is treated in 2.1.

As outlined in the introduction, the fluid and the solid domain of a FSI problem might be described by means of many different models: some of them are outlined in section 2.2. *Dimensional analysis* and the use of dimensionless numbers is a powerful tool used to classify fluid dynamics problems: some of the principles used there can be applied to FSI problems in order to classify them: this can help define and classify FSI problems, as described in section 2.3.

### 2.1 Description of motion

In a FSI model, the fluid in motion deforms the solid because of the forces exerted to the structure. The change in the shape of the solid modifies the fluid domain, causing a different flow behavior. For this reason it is necessary to describe formally the kinematics and the dynamics of the whole process. Classical continuum mechanics considers the motion of particles by means of two different perspectives [2]: the *Eulerian description*, briefly described in section 2.1.1, and the *Lagrangian description*, outlined in section 2.1.2. Those two perspectives are typically combined into the *arbitrary Lagrangian-Eulerian (ALE)* method, described in section 2.1.3.

#### 2.1.1 Eulerian perspective

The *Eulerian perspective* observes the change of quantities of interest (e.g. density, velocity, pressure) at spatially fixed locations. In other words: the observer does not vary the point of view during different time steps. Thus, quantities can be expressed as functions of time at fixed locations. This is represented by the following notation:

$$\Theta = \tilde{\Theta}(x, y, z, t) \tag{2.1}$$

where  $\Theta$  is a quantity of interest and  $\tilde{\Theta}$  denotes the same quantity from an Eulerian point of view;  $(x, y, z)$  represent a fixed location in the euclidean space.

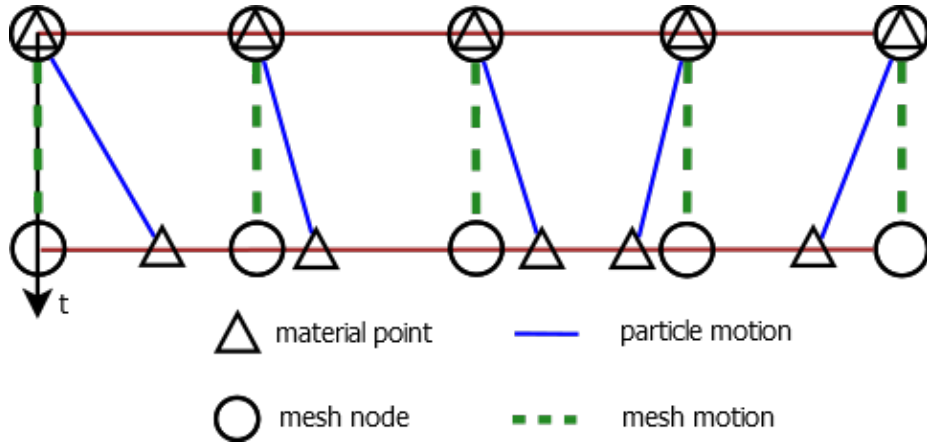


Figure 2.1. Eulerian perspective

A computational mesh can be interpreted as a number of observers distributed across the domain of interest and connected to each other in order to form a grid with nodes. If the particles of the domain move, a purely euclidean mesh does not move and the position other nodes remain fixed at any instance of time [3]. This behavior is represented in Figure 2.1 (adapted from [3]). The mesh is independent of particles movement, resulting in a convenient choice for Computational Fluid Dynamics (CFD) problems, where fluid flows throughout the whole computational domain. Within this approach, proper mesh refinement is crucial for computational accuracy as it defines to what extent small scale movement can be modeled and resolved [4].

### 2.1.2 Lagrangian perspective

A *lagrangian observer* focuses on a single particles and follows it throughout the motion, as depicted in Figure 2.2. Changes in the quantities of interest are observed at different spatial locations.

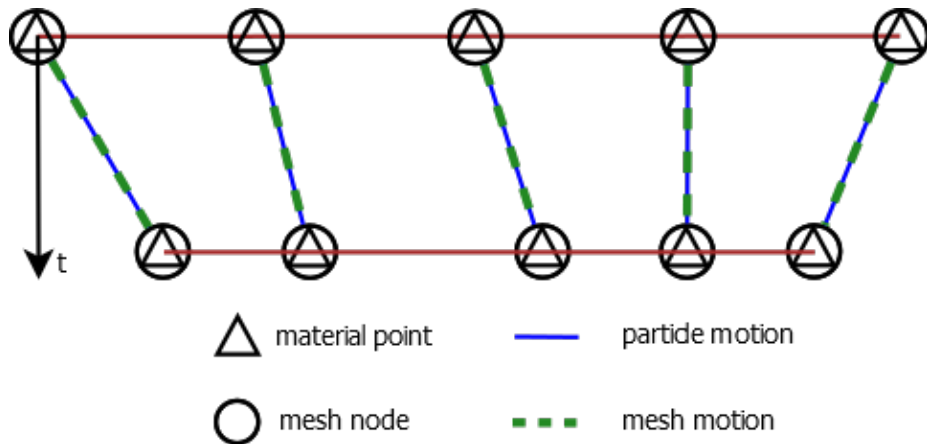


Figure 2.2. Lagrangian perspective

The motion of the particle and the other quantities of interest can be described by reference coordinates (or *material coordinates*) in Euclidean space  $(X, Y, Z)$ , uniquely identifying the observed particle at a reference configuration [5]. Usually  $t = 0$  is chosen as reference but this

is not mandatory. The Lagrangian observer only registers changes concerning one specific particle as time advances. Thus, quantities of interest can be described as:

$$\Theta = \hat{\Theta}(X, Y, Z, t) \quad (2.2)$$

In contrast to the Eulerian perspective (Equation 2.1), the obtained information is strictly limited to a single material particle (implied by the usage of the capital reference coordinate variables). Information about a fixed point in space is not directly available and no convective fluxes appear in a Lagrangian description.

This perspective is again translated into computational meshes: at a reference instance of time, mesh nodes are attached to material particles. As these move, the mesh nodes move with them causing the mesh to deform. Figure 2.2 describes the situation. The mesh nodes always coincide with their respective particles.

In this situation large-scale and irregular motions and more importantly deformation lead to distortions of the computational mesh, which yields smaller accuracy in simulations requiring to apply techniques to keep the desired accuracy [6].

Lagrangian perspective is the usual method of choice for Computational Solid Mechanics (CSM) simulations.

Eulerian and Lagrangian descriptions are related [7]. A mapping between them can be described by the *motion* function  $\phi$  such that:

$$\vec{x}(t) = \phi(\vec{X}, t) \quad (2.3)$$

Equation 2.3 tells that the Eulerian, spatial position  $\vec{x}$  of a particle at time  $t$  is the mapping of the particle at its reference configuration  $\vec{X}$ : the mapping must be bijective.

### 2.1.3 ALE method

As outlined above, CSM and CFD problems adopt different perspectives. The ALE approach, a combination of the two points of view, is used for FSI problems. As the name implies, an ALE observer moves arbitrarily with respect to a specific material particle. Figure 2.3 depicts such a situation.

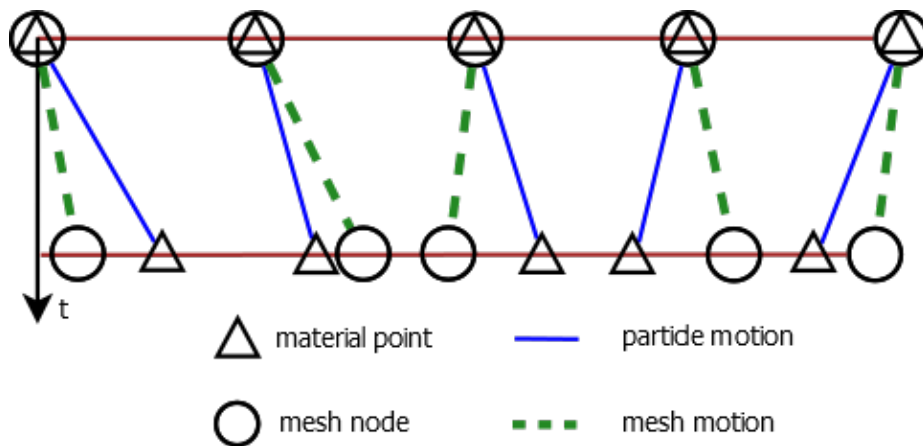
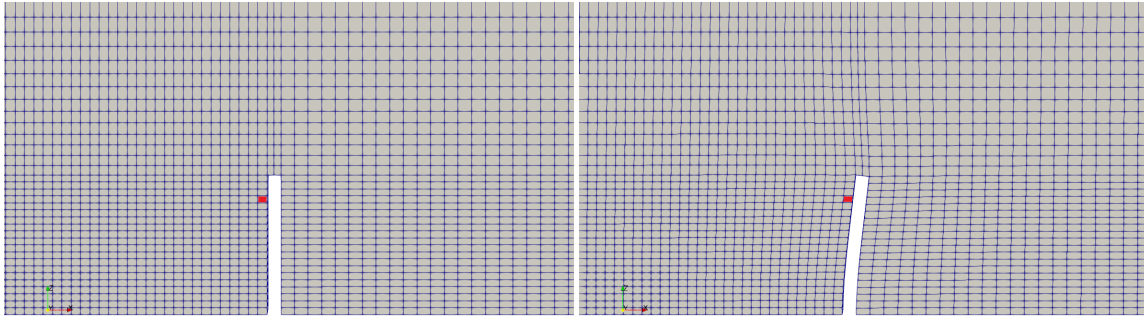


Figure 2.3. ALE perspective

When dealing with computational meshes, an ALE mesh is considered as it can move almost arbitrarily with respect to the motion of the underlying particles, as shown in Figure 2.4. The only constraint is that node movements should not distort the mesh too much

as this leads to computational inaccuracy. Many algorithm exist to implement suitable quality criteria and keep the mesh motion reasonable and to allow the nodes to follow moving particles up to a certain extent [8].

Since the mesh motion and material particle motion are not directly linked, a new unknown is introduced: the relative movement between the ALE mesh and the material domain. This approach is particularly useful in FSI problems: fluid and solid must follow the moving interface between them for physical reasons. Since the solid domain is usually described in a Lagrangian perspective, the solid mesh is kept attached to the FSI interface. However, also the fluid domain must deform to avoid formation of gaps between the meshes. Therefore, in ALE methods the fluid mesh nodes at the interface move with it. Fluid mesh nodes follow the fluid particles sticking to the interface (for viscous flows), while the rest of the fluid mesh is allowed to move in such way that mesh distortions are kept minimal, to preserve computational accuracy [9].



(a) undistorted mesh

(b) distorted mesh

Figure 2.4. ALE mesh

## 2.2 Domains and interface

Fluid-structure interaction implies that the overall model is determined by models defining the fluid behavior and the solid behavior, briefly described in sections 2.2.2 and 2.2.1. A short overview of beam models is given in section 2.2.3 as it is relevant for the model developed in this work. Finally a formal definition of the interface is given in section 2.2.4, as it is necessary to define suitable coupling conditions at the common boundary of the solid and the fluid.

### 2.2.1 Fluid domain

An exhaustive description of all possible fluid models is far beyond the scope of this work. A quite general model is the viscous compressible one described by the Navier Stokes Equations (NSE).

$$\frac{\partial \rho}{\partial t} + \nabla \cdot (\rho \vec{v}) = 0 \quad (2.4a)$$

$$\frac{\partial}{\partial t} (\rho \vec{v}) + \nabla \cdot (\rho \vec{v} \otimes \vec{v}) + \nabla p - \nabla \cdot \tau - \rho \vec{g} = 0 \quad (2.4b)$$

$$\frac{\partial}{\partial t} (\rho e_0) + \nabla \cdot (\rho e_0 \vec{v}) + \nabla \cdot (\vec{v} p + \vec{q} - \vec{v} \cdot \tau) - \vec{v} \cdot \rho \vec{g} = 0 \quad (2.4c)$$

where:

- $\rho$  denotes density
- $\vec{v}$  is flow velocity in all dimensions
- $p$  denotes pressure
- $\boldsymbol{\tau}$  is the viscous stress tensor
- $\vec{g}$  represents the sum of all body forces
- $e_0$  is the total energy per unit mass
- $\vec{q}$  is the heat flux by conduction

They consist in the mass conservation equation (2.4a), the conservation of momentum equation (2.4b) and the energy conservation equation (2.4c). For a Newtonian fluid, the viscous stress tensor is given by:

$$\boldsymbol{\tau} = -\frac{2}{3}\mu (\nabla \cdot \vec{v}) \boldsymbol{I} + 2\mu \boldsymbol{S} \quad (2.5)$$

with  $\mu$  being the dynamic viscosity and  $\boldsymbol{S}$  the rate of deformation tensor (i.e. the symmetric part of the velocity gradient  $\nabla \vec{v}$ ):

$$\boldsymbol{S} = \frac{1}{2} (\nabla \vec{v} + \nabla \vec{v}^T) \quad (2.6)$$

A detailed derivation of such equations and the theory beyond can be found for example in [10] and [11] or in [12].

The set of equations above, even with a Newtonian fluid model, lack some other information in order to form a closed set of Partial Differential Equations (PDE). A conductive heat flux model is needed (e.g. Fourier's Law), the caloric and thermodynamic equations of state have to be chosen, a proper turbulence model if needed (see [12]) and finally, the appropriate initial and boundary conditions for the problem [13] must be defined.

Simplifications can be done to obtain less sophisticated models such as: adiabatic, inviscid, incompressible, and many others. Dimensional Analysis is a powerful tool to determine to what extent some reduced models are meaningful, and it is widely used in fluid dynamics, as described in section 2.3.1. Most CFD software codes allow to set up simulations with the most suitable model which can be coupled with a solid model to build a FSI problem. Some further details are given in section 3.1.

### 2.2.2 Solid domain

In solid mechanics, particles do not travel as much as they do in fluid dynamic problems, as described in 2.1.2. For this reason, a Lagrangian perspective is generally used.

The de-Saint Venant-Kirchhoff model [14] is very commonly used when describing the movement of a solid: it is also often used in FSI problems as it is capable of handling large deformation. The material is considered:

- *homogeneous*: the material properties do not depend on the position of the particle
- *linear elastic*: the stress-strain relationship is linear
- *isotropic*: the stress-strain relationship is independent from the direction of the load

A general expression of the dynamic equation can be derived from the Virtual Work Principle (VWP) applied to an arbitrary control volume:

$$\frac{\partial^2 \vec{u}}{\partial t^2} = \nabla \cdot \mathbf{T} + \rho \vec{f} \quad (2.7)$$

In equation 2.7:

- $\rho$ : is the material density
- $\vec{u}$ : is the particle displacement
- $\mathbf{T}$ : is the *second Piola-Kirchhoff* stress tensor
- $\vec{f}$ : is the sum of body forces

In order to close the dynamic equation, a constitutive law which must be considered to relate stress and strain:

$$\mathbf{T} = \lambda \mathbf{I} \text{tr} [\boldsymbol{\varepsilon}_G] + 2\mu \boldsymbol{\varepsilon}_G \quad (2.8)$$

where  $\boldsymbol{\varepsilon}_G$  is the Green-Lagrange strain tensor:

$$\boldsymbol{\varepsilon}_G = \frac{1}{2} (\mathbf{F}^T \mathbf{F} - \mathbf{I}) \quad (2.9)$$

and  $\mathbf{F}$  is the deformation gradient.  $\lambda$  and  $\mu$  are material properties and are named Lamé constants. These relate to the Young modulus  $E$  and the Poisson ratio  $\nu$  which are more commonly used in practice. The relationship among the various parameters is the following:

$$E = \frac{\mu(3\lambda + 2\mu)}{\lambda + \mu} \quad (2.10)$$

$$\nu = \frac{\lambda}{2(\lambda + \mu)} \quad (2.11)$$

The set of parameters  $(E, \nu)$  or  $(\lambda, \mu)$ , together with the density  $\rho$  fully define the material, under the assumptions of linear elasticity, isotropy and homogeneity.

The set of PDEs is completed when suitable initial and boundary conditions are defined.

### 2.2.3 Models with reduced dimensionality: beams

The equations introduced in section 2.2.2 may be a tough task to solve even of the case of isotropic hyperelasticity, when considering a 3-D domain. Even with today's computers and using finite elements techniques, it is not always feasible or convenient to treat a solid as a three-dimensional continuum. Body with particular geometric features can be seen as lower dimension bodies, with respect to the governing equations [15]. Such bodies are called *beams* (one dimension) , *plates* or *shells* (two dimensions).

The *beam* model splits the description of the geometry into two subproblems:

1. a beam is defined by its *reference line* and the movement (displacement and rotation) of the solid is completely defined by it (see Figure 2.5),

- the beam *cross section* is considered as a whole, its movement depends on the movement of the reference line, stresses are generalized into *resultants* (axial, bending, shear, torsional) which represent the aggregate effect of all of the stresses acting on the cross section. The constitutive properties of the section (axial, shear, torsion and bending stiffness) allow to relate stresses and deformations (by means of VWP) and close the problem.

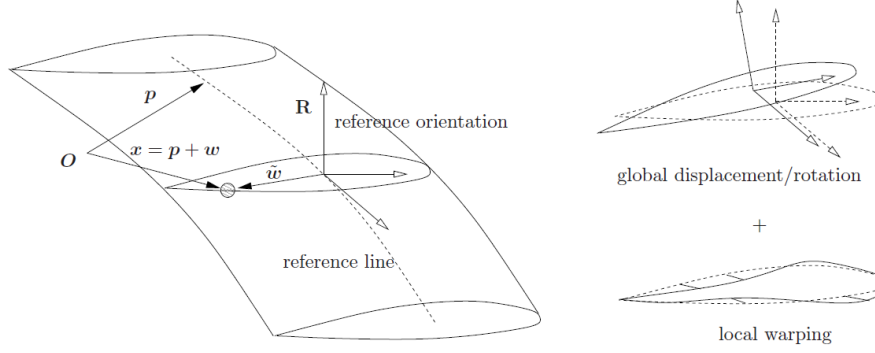


Figure 2.5. beam model, taken from [1]

The beam model can be used to build elements of a Finite Element Method (FEM). For example, the beam element can be modeled by means of a Finite Volume approach, as described in [16], which computes the internal forces as functions of the straining of the reference line and orientation at selected points along the line itself, called evaluation points.

This approach is particularly interesting for FSI problems in which slender structures are involved. A mapping is needed between the fluid-solid interface and the reference line movement, which will be described in.

#### 2.2.4 Interface and interaction

Since FSI problems are centered on the interaction of the fluid and solid domain, their common interface needs to be described properly. A simple representation of the situation at the so called *wet surface* is shown in Figure 2.6. Quantities related to the solid use S subscript, while fluid domain and the interface are labeled with F and FS, respectively.

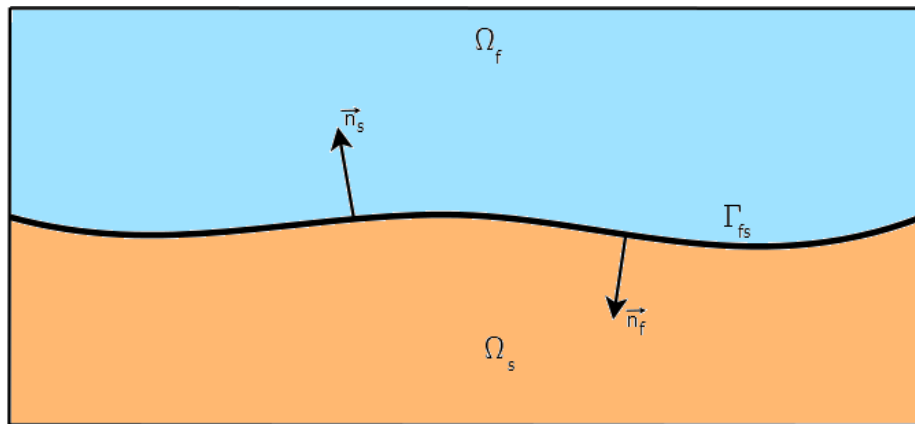


Figure 2.6. fluid solid interface

In order to have a physically correct behavior, some conditions have to be met [17]:

- solid and fluid domains should not overlap nor separate,
- for a viscous fluid model, the flow velocity at the interface must equal the boundary velocity (*no-slip* condition),
- for an inviscid fluid model, only velocity components normal to the wet surface have to be equal to the structural velocity as the fluid may slip freely in tangential direction at any boundary,
- forces exchanged at the interface must at equilibrium.

The first conditions result in the *kinematical requirement* that the displacements of fluid and solid domains, as well as their respective velocities have to be equal at the wet surface (denoted by  $\Gamma_{FS}$ ):

$$\Delta \vec{x}_F = \vec{u}_S \quad (2.12)$$

$$\vec{v}_F = \frac{\partial \vec{u}_S}{\partial t} \quad (2.13)$$

The last condition results in the equilibrium requirement. Force vectors are computed from the stresses at the interface and the outward normal vectors of fluid and solid domain, respectively. They have to be equal and opposite leading to the dynamic coupling condition:

$$\boldsymbol{\sigma}_F \cdot \vec{n}_F + \boldsymbol{\sigma}_S \cdot \vec{n}_F = 0 \quad (2.14)$$

$\boldsymbol{\sigma} \in \mathbb{R}^{3 \times 3}$  represents the stress tensor (note that for the fluid it comprises pressure and viscous stresses), while  $\vec{n} \in \mathbb{R}$  is the outward normal unit vector.

## 2.3 Classification of FSI problems

In the previous chapters we have seen that there exist a lot of models that can describe fluid flow and solid mechanics. In FSI problems we need to couple two of them: the variety of coupled problems seems to be so large that single FSI model that is applicable to every problem appears to be unfeasible. For this reason it is useful to classify FSI problems and look for specific properties in each class. The first step is to switch from dimensional quantities to dimensionless ones.

### 2.3.1 Dimensional analysis

We use the principle that a physical law should only relate to dimensionless quantities. There exist a rather general theorem called the  $\Pi$  Theorem or the *Vaschy-Buckingham Theorem* [18], which tells how many dimensionless quantities are needed to rewrite a model in dimensionless fashion. This theorem states that the number of dimensionless quantities,  $P$ , is equal to that of the dimensional ones describing the problem,  $N$ , minus  $R$ , which is the rank of the matrix of dimension exponents. This matrix is formed by the columns of the dimension exponents of all variables [19]. An example is given in the following Section 2.3.2, Table 2.1.



### 2.3.2 Dimensional analysis in fluid domain

Dimensional analysis is widely used in fluid dynamics. In order to keep the analysis simple, we consider the adimensionalization of the incompressible Navier-Stokes momentum equation for a Newtonian fluid [20]:

$$\frac{\partial \vec{v}}{\partial t} + (\vec{v} \cdot \nabla) \vec{v} = -\frac{\nabla p}{\rho} + \nu \nabla^2 \vec{v} + \vec{g} \quad (2.15)$$

The variables involved in equation 2.15 are the following:

- $t$ : time
- $\vec{x}$ : coordinates
- $\vec{v}$ : velocity field
- $p$ : pressure field
- $\rho$ : fluid density
- $\nu$ : fluid kinematic viscosity
- $\vec{g}$ : gravity
- $L$ : reference dimension
- $V_0$ : reference velocity

	$t$	$\vec{x}$	$\vec{v}$	$p$	$\rho$	$\nu$	$\vec{g}$	$L$	$V_0$
L	0	1	1	-1	-3	2	1	1	1
M	0	0	0	1	1	0	0	0	0
T	1	0	-1	-1	0	-1	-2	0	-1

Table 2.1. fluid matrix of dimension exponents

The rank of the above matrix is 3 so 6 dimensionless parameters are needed to rewrite the equation 2.15:

- *length*:  $\vec{x}^* = \frac{\vec{x}}{L}$
- *velocity*:  $\vec{v}^* = \frac{\vec{v}}{V_0}$
- *time*:  $t^* = \frac{V_0 t}{L} = \frac{t}{T_{fluid}}$
- *pressure*: possible choices:  $p^* = \frac{p}{\rho V_0^2}$  or, if viscous forces are dominant,  $p^* = \frac{pL}{\rho \nu V_0}$
- *Reynolds number*:  $Re = \frac{V_0 L}{\nu}$ . It defines the ratio between inertia and viscous forces.
- *Froude number*:  $Fr = \frac{V_0}{\sqrt{gL}}$ . It defines the ratio between the flow inertia to the body field forces

The adimensionalized momentum equation becomes:

$$\frac{\partial \vec{v}^*}{\partial t^*} + (\vec{v}^* \cdot \nabla) \vec{v}^* = -\nabla p^* + \frac{1}{Re} \nabla^2 \vec{v}^* + \frac{1}{Fr^2} \vec{g} \quad (2.16)$$

From Equation 2.16 a lot of models might be derived: from *Stokes regime* when viscosity is dominant, to *Euler regime* when viscosity is negligible with respect to inertia forces.

### 2.3.3 Dimensional analysis in solid domain

Even if it is seldom used, Dimensional Analysis can be made also for the solid domain [21].

The variables involved in a solid dynamics equation are:

- $t$ : time
- $\vec{X}$ : coordinates
- $\vec{u}$ : displacement field
- $\rho_S$ : solid density
- $E$ : elastic modulus
- $\vec{g}$ : gravity
- $L$ : reference dimension
- $U_0$ : reference displacement

From the variables above the following parameters can be derived:

- *length*:  $\frac{\vec{X}}{L}$ : dimensionless coordinate
- *displacement*:  $\frac{\vec{u}}{L}$ : dimensionless displacement
- *time*:  $\frac{t\sqrt{\frac{E}{\rho_S}}}{L} = \frac{t}{T_{solid}}$  dimensionless time
- entity of displacements:  $\frac{U_0}{L} = \delta$ : *displacement number*
- gravity:  $\frac{\rho_S g L}{E}$ : elastogravity number

$T_{solid}$  can be seen as  $\frac{L}{c}$  with  $c = \sqrt{\frac{E}{\rho_S}}$  which is the scale of elastic wave velocity. The displacement number  $\delta$  tells how big the structure displacement are related to the overall dimension, and defines the *large displacements* region. Finally, the *elastogravity number* combines gravity (or body forces in general), density and stiffness: when large the deformation induced by body forces in the solid are large.

### 2.3.4 Dimensional analysis of coupled problems

It is now possible to undertake the dimensional analysis of a fully coupled fluid and solid interaction problem. Some of the parameters are only defined in the fluid side or in the solid side (e.g. viscosity or stiffness). Some parameters are common to both domains (e.g. length scale or gravity). The variables of interest are now the velocity in the fluid and the displacements in the solid. Each of them can be related to all the parameters without separation. For example, the fluid velocity relationship is of the kind:

$$g(\vec{v}; \vec{x}, t; \rho, \mu, V_0; \rho_S, E; \vec{g}, L) = 0 \quad (2.17)$$

Equation 2.17 is composed of 11 dimensional parameters. Applying  $\pi$  theorem, the total number of independent dimensionless parameter expected is 8. Starting from the ones derived in the previous sections:

- $\vec{x}^* = \frac{\vec{x}}{L}$ : dimensionless coordinates
- $\vec{v}^* = \frac{\vec{v}}{V_0}$ : dimensionless fluid velocity
- $t^*_f = \frac{V_0 t}{L}$ : dimensionless time
- $Re = \frac{V_0 L}{\nu}$ : Reynolds number
- $Fr = \frac{V_0}{\sqrt{gL}}$ : Froude number
- $\delta = \frac{U_0}{L}$ : displacement number
- $\frac{\rho_s g L}{E}$ : elastogravity number

The 7 quantities above derive from the separated problem. The last one necessarily mixes things from the fluid and the solid side otherwise it would have been found in one uncoupled case. There is no unique choice for this parameter, the following are the most common ones.

### Mass number

The simplest, but arguably most important parameter is the ratio of the two densities: the *Mass Number*  $M$ .

$$M = \frac{\rho}{\rho_s} \quad (2.18)$$

This can range from  $\mathcal{O}(10^{-4})$  in air-steel interaction to  $\mathcal{O}(1)$  when both media have about the same density. This parameter is particularly significant for the so called *added mass* stability problem, described in Section 3.5.

### Reduced velocity

Another possible choice is the reduced velocity:

$$U_R = \frac{V_0}{\sqrt{\frac{E}{\rho_s}}} \quad (2.19)$$

It is the ratio between the fluid free velocity and the velocity of elastic waves in a solid,  $c$ . It contains information on the way the two dynamics are related and it can range different orders of magnitude.

### Cauchy number

Another possible parameter combines stresses or stiffness: the Cauchy number, as defined in [22]:

$$C_Y = \frac{\rho V_0^2}{E} \quad (2.20)$$

It is the ratio between the fluid inertial forces, quantified by the dynamic pressure and the stiffness of the solid  $E$ . The higher it is, the more the solid is elastically deformed by the flow.

These are actually the most important parameters involving FSI problems. Among them, there is no universally better choice. But there are efficient choices, that would be more helpful in solving a given problem.



## Chapter 3

# Computational aspects of Fluid-Structure Interaction problems

This section deals with the computational aspects of FSI problems. The first possible categorization of solution techniques distinguishes between monolithic and partitioned approach, as discussed in Section 3.1. This work is based on the latter approach, so the two different coupling strategies, namely strong and weak, are discussed in Section 3.2. As strong coupling is generally needed for accurate solution, an overview of strong coupling algorithms is given in Section 3.3. Section 3.4 focuses on aspects concerning the interface mesh, and how the solid and the fluid exchange data between them. Finally 3.5 briefly describes a common issue arising in strongly coupled problems: the added mass effect (AME).

### 3.1 Monolithic and Partitioned Approach

Analytical solutions are impossible to obtain for the large majority of FSI problems; on the other hand, laboratory experiments may be costly, unfeasible or limited. For those reasons, numerical simulations may be employed to analyze the physics involved in the interaction between fluids and solids. With the current capabilities of computer technology, simulations of scientific and engineering models have become increasingly detailed and sophisticated.

The numerical methods used to solve FSI problems may be roughly classified into two classes: the *monolithic approach* and the *partitioned approach*. There is no exact distinction between the two approaches, as they might be seen differently among fields of applications. The idea here is to consider how many solvers are used to find a solution.

In the *monolithic approach*, the whole problem is treated as a unique entity and solved simultaneously with a specialized ad hoc solver (see Figure 3.1). The fluid and structure dynamics form a single system of equations for the entire problem, which is solved simultaneously by a unified algorithm. The interface conditions are implicit in the solution procedure [23], [24].

This approach can potentially achieve better accuracy, as they solve the system of equations exactly the interface conditions are implicit in the model [25], but it may require more resources and expertise to develop from scratch a specialized code (it solves a very specific model) that can be cumbersome to maintain.

On the other hand, in the *partitioned approach*, the fluid and the solid domains are treated as two distinct computational fields, with their respective meshes, that have to be solved separately (see Figure 3.2: how data are passed between solvers is detailed in Section 3.2). The interface conditions are used explicitly to communicate information between the

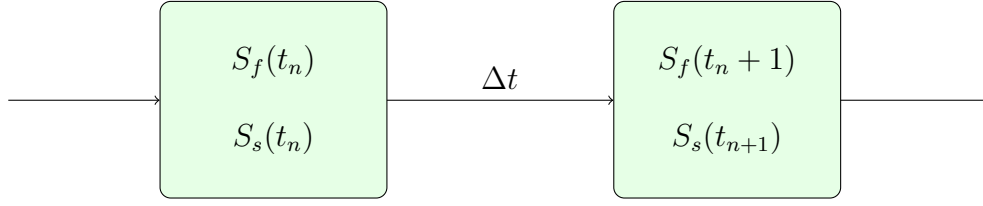


Figure 3.1. monolithic approach:  $S_f$ ,  $S_s$  denote the fluid and the structure solutions

fluid and structure solutions. This implies that the flow does not change while the solution of the structural equations is calculated and vice versa [26]. The partitioned approach thus requires a third software module (i.e. a coupling algorithm) to incorporate the interaction aspects. It communicates the boundary conditions described in Section 2.2.4: that is forces or stresses (dynamic data) calculated by the fluid solver at the wet surface are passed to the solid component and displacements or velocities (kinematic data) computed by the solid solver at the interface are sent to the fluid component in return. Finally, fluid and structural solutions together yield the FSI solution.

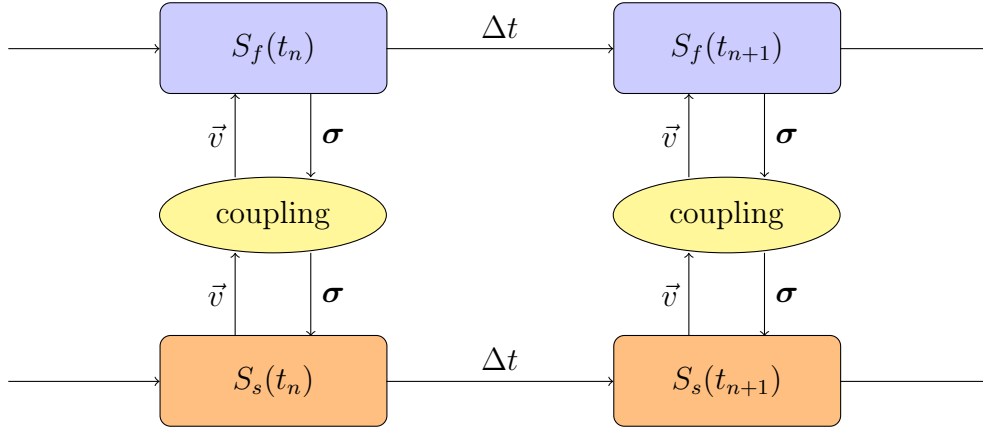


Figure 3.2. partitioned approach:  $S_f$ ,  $S_s$  denote the fluid and the structure solutions, while  $\sigma$  and  $\vec{v}$  represent coupling data

A big advantage of this approach is that software modularity is preserved: different and efficient solution techniques can be used for the flow equations and structural equations. Provided that they can exchange data, existing solvers for the fluid and solid problem can be reused, ranging from commercial to academic and open-source codes. Those solvers are usually well-validated. Besides, compared to monolithic procedures, the programming efforts are lower for partitioned approaches, as only the coupling of the existing solvers has to be implemented rather than the solvers themselves. The challenge of this approach is, however, to define and implement algorithms to achieve accurate and efficient fluid-structure interaction solution with minimal code modification. Particularly, the interface location that divides the fluid and the structure domains changes in time. The partitioned approach requires that the fluid solver has ALE capabilities, as introduced in Section 2.1.3. More detailed and practical explanations about the coupling component used in this work are given in Section 4.1.

## 3.2 Coupling Strategies

Because of the modularity, the partitioned approach has gained much attention in research. The structure sketched in Figure 3.2 needs to be detailed and specialized in function of the coupling strategies.

In an interface multi-physics coupling like FSI, the boundary surface is in common between the two sides of the simulation. The results make sense and are numerically stable only if the two sides of the interface are in agreement, since the output values of the one simulation become input values for the other (and vice-versa). The solution strategies can be roughly divided into weakly and strongly coupled approaches. They are often referred to as *explicit* and *implicit* methods in the literature. When the fluid and solid solutions are computed iteratively until some convergence criteria within the same time step, the scheme is called *implicit coupling*. The faster, simpler but less precise *explicit coupling* consists in executing a fixed number of iterations (typically one per time step) and exchange coupling values without convergence checks.

### 3.2.1 Explicit coupling schemes

As in the previous Section,  $S_f$  represents the fluid solver, which computes the pressures (named  $d_f$  here) at the deformable boundary and  $S_s$  is the structure solver, which uses these forces to compute the displacement and velocity of the boundary (named  $d_s$ ). In a *serial-explicit* (or *conventional staggered*) coupling scheme, the solver  $S_f$  uses the old time step boundary values  $d_s^{(n)}$  to compute the values of  $d_f^{(n+1)}$  for the next time step:

$$d_f^{(n+1)} = S_f \left( d_s^{(n)} \right) \quad (3.1)$$

When the fluid solver completes the time step, data are passed to the structural solver:

$$d_s^{(n+1)} = S_s \left( d_f^{(n+1)} \right) \quad (3.2)$$

Note that Equation 3.1 uses values computed at  $t^n$ , while Equation 3.2 uses values computed at  $t^{(n+1)}$ . The order of execution might be inverted.

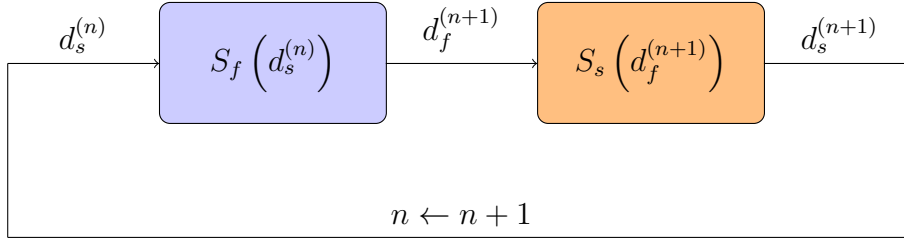
In order to reduce execution time, the solvers might run in parallel, using data from the same time step (*parallel-explicit coupling*):

$$d_f^{(n+1)} = S_f \left( d_s^{(n)} \right) \quad (3.3a)$$

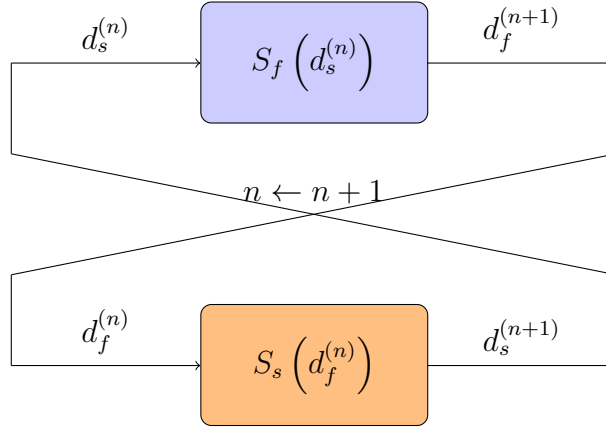
$$d_s^{(n+1)} = S_s \left( d_f^{(n)} \right) \quad (3.3b)$$

The two explicit schemes are shown schematically in Figures 3.3a and 3.3b.

In general, an explicit coupling is not enough to regain the exact (as in the monolithic approach) solution of the problem as the matching coupling conditions between the solvers is not enforced within each time step: no balance between fluid and structural domain with respect to forces and displacements at the interface can be guaranteed ([17], [26]). Nevertheless, explicit coupling yields good results if the interaction between fluid and solid is weak as in aeroelastic simulations, where in general the simulations show small displacements of the structure within a single time step and the flow field isn't much influenced by the structural displacements ([27]).



(a) serial explicit coupling



(b) parallel explicit coupling

Figure 3.3. Explicit coupling schemes

### 3.2.2 Implicit coupling schemes

On the other hand, strongly (implicit) coupling techniques require an iterative method to solve the fixed-point equation that derives from enforcing the agreement of the interface variables. The coupling conditions at the wet surface are enforced in each time step up to a convergence criterion. If the criterion is not met, another subiteration within the same time instance is computed. Therefore, the solution can approximate the monolithic solution to an arbitrary accuracy.

As in the explicit case, solvers may run in a sequential mode: the coupling is then named *serial* (or staggered) and the solvers wait for each other.

$$d_f^{(n+1),i+1} = S_f(d_s^{(n+1),i}) \quad (3.4a)$$

$$d_s^{(n+1),i+1} = S_s(d_f^{(n+1),i+1}) \quad (3.4b)$$

Equations 3.4 show that, in contrast with explicit coupling, both solvers use interface values at time step  $n + 1$ , but one of them uses data from previous iteration. If run in parallel mode [28], the system becomes:

$$d_f^{(n+1),i+1} = S_f(d_s^{(n+1),i}) \quad (3.5a)$$

$$d_s^{(n+1),i+1} = S_s(d_f^{(n+1),i}) \quad (3.5b)$$



At convergence, the following relation holds of serial (or *Gauss-Seidel*) coupling:

$$d_s^{(n+1)} = S_s \left( S_f \left( d_s^{(n+1)} \right) \right) \quad (3.6a)$$

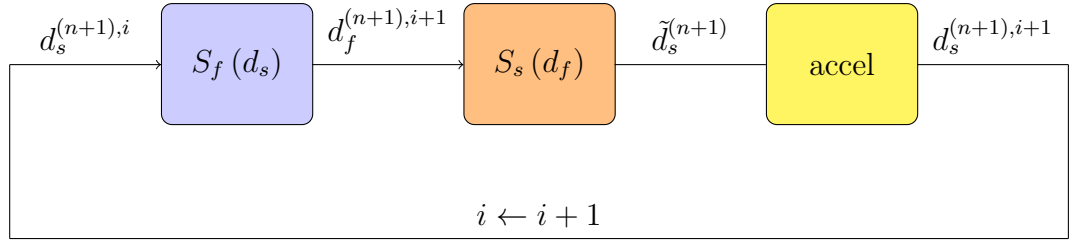
$$d_s^{(n+1)} = S_s \circ S_f \left( d_s^{(n+1)} \right) \quad (3.6b)$$

and the following relation holds for parallel (or *Jacobi*) coupling:

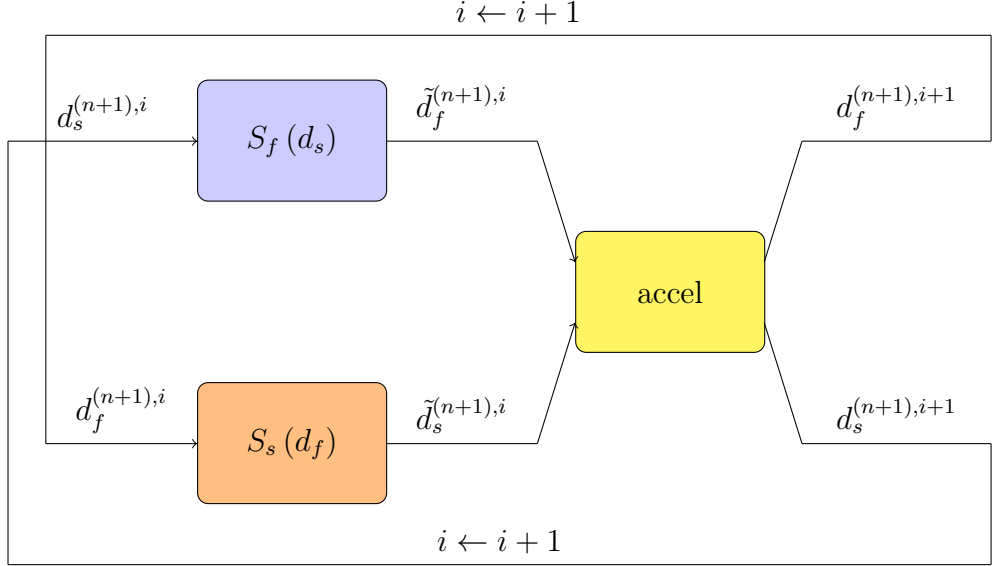
$$\begin{pmatrix} d_s^{(n+1)} \\ d_f^{(n+1)} \end{pmatrix} = \begin{pmatrix} 0 & S_f \\ S_s & 0 \end{pmatrix} \begin{pmatrix} d_s^{(n+1)} \\ d_f^{(n+1)} \end{pmatrix} \quad (3.7)$$

Acceleration techniques are necessary to bring fixed point equation 3.6b or 3.7 to convergence. Those techniques are described in Section 3.3.

The two implicit schemes are shown schematically in Figures 3.4a and 3.4b: *accel* refers to the post-processing step implemented to speedup convergence. After every non-converged iteration, the latest stored state of the solver (*checkpoint*) is reloaded and coupling iteration  $i$  for the current time step is incremented. When the solution converges, the time step  $n$  is incremented.



(a) serial implicit coupling



(b) parallel implicit coupling

Figure 3.4. Implicit coupling schemes

Implicit methods are generally applicable to any kind of FSI problems, in contrast with explicit methods. When fluid and structure are strongly coupled, explicit coupling can be

subject to numerical instabilities, a problem that cannot always be solved by reducing the coupling time step size [29]. These instabilities can be overcome by implicit methods, even if several coupling iterations may be executed every time step, until the values on both sides of the interface converge.

### 3.3 Strong coupling algorithms

As mentioned in the previous section, implicit methods require some post-processing (generally called *acceleration*) techniques to make the solution of the single time step of the coupled partitioned FSI problem converge. This requires to solve a *fixed-point equation*, in fact:

$$H(d_s) := S_s \circ S_f(d_s) \quad (3.8a)$$

$$d_s = H(d_s) \quad (3.8b)$$

$$R(d) := H(d) - d = 0 \quad (3.8c)$$

Equation 3.8a represents the composition of the solid and the fluid solution, while Equation 3.8b represents the resulting fixed point equation. As the order of execution can be switched, in Equation 3.8c, where the *residual* is defined, the input data  $d_s$  is generically substituted with  $d$ .

The basic approach to solve the fixed point equation is to perform the corresponding fixed point iteration (**FPI**):

$$x_{i+1} = H(x_i) \quad i = 1, 2, \dots \quad (3.9)$$

which is known to converge if the mapping  $H$  is a contraction, but this is not the general case in FSI computations [28].

#### 3.3.1 under-relaxation

The way to stabilize the iterations is to perform a FPI with *under-relaxation* as illustrated in the following algorithm:

---

**Algorithm 1:** FPI with relaxation

---

**Result:**  $d_k$

```

1 initialization of  $d_0$ ;
2  $k = 0$ ;
3  $\tilde{d}_1 = S_s \circ S_f(d_0)$ ;
4  $r_0 = \tilde{d}_1 - d_0$ ;
5 while  $\|r_k\| > \varepsilon$  do
6   | compute  $d_k$  by relaxation;
7   |  $k = k + 1$ ;
8 end
```

---

The under-relaxation is defined by:

$$d_{k+1} = d_k + \omega (H(d_k) - d_k) \quad (3.10)$$

Where  $\omega$  in Equation 3.10 is the *relaxation factor*. The relaxation parameter has to be small enough to keep the iteration from diverging, but as large as possible in order to use as

much of the new solution as possible [30]. The optimal  $\omega$  value is problem specific and not known a priori. A suitable dynamic relaxation parameter, is a better choice, like the *Aitken under-relaxation* [31] which adapts the factor at each iteration with the following relation:

$$\omega_i = -\omega_{i-1} \frac{r_{i-1}^T (r_i - r_{i-1})}{\|r_i - r_{i-1}\|^2} \quad (3.11)$$

Aitken under-relaxation can be a good choice for strong interaction with a fluid solvers that does not fully converge in every iteration or for compressible fluid solvers.

### 3.3.2 Quasi Newton Least Squares schemes

Under-relaxation is a good choice for easy stable problems, but is outperformed by more sophisticated quasi-Newton coupling schemes. Equation 3.8c could be solved iteratively with a Newton method [32]:

$$R(d_k) \quad := \quad r_k \quad (3.12a)$$

$$R(d_k) + \left. \frac{\partial R}{\partial d} \right|_{d_k} (d_{k+1} - d_k) = 0 \quad (3.12b)$$

$$d_k + \left( \left. \frac{\partial R}{\partial d} \right|_{d_k} \right)^{-1} (-r_k) = d_{k+1} \quad (3.12c)$$

The *residual* at iteration  $k$  is defined in Equation 3.12a, if the Jacobian matrix of the equation is known, a Newton iteration can be performed as in Equation 3.12b. The updated values can be computed using Equation 3.12c.

In situations where:

- *black-box* systems are considered (i.e. the Jacobian is unknown),
- the cost of a function evaluation is sufficiently high that numerical estimation of the Jacobian is prohibitive,

there exist a number of matrix-free methods that use only information derived from the consecutive iterates and that build an approximation based on those values. This approach is known as *quasi-Newton method* [33]. Input and output data of  $H$  and  $R$  are used to approximate the solution of 3.12c. Algorithm 12 (taken from [34]) shows the basics steps to

estimate data at next step using the *Quasi Newton Least Squares Method*:

---

**Algorithm 2:** Quasi Newton Least Squares method
 

---

**Result:**  $d_{k+1}$

- 1 initial value  $d_0$ ;
- 2  $\tilde{d}_0 = H(d_0)$  and  $R_0 = \tilde{d}_0 - d_0$ ;
- 3  $d_1 = d_0 + \omega r_0$ ;
- 4 **for**  $k = 1 \dots$  **do**
- 5      $\tilde{d}_k = H(d_k)$  and  $r^k = \tilde{d}_k - d_k$ ;
- 6      $V^k = [\Delta r_0^k, \dots, \Delta r_{k-1}^k]$  with  $\Delta r_i^k = r^i - r^k$ ;
- 7      $W^k = [\Delta \tilde{d}_0^k, \dots, \Delta \tilde{d}_{k-1}^k]$  with  $\Delta \tilde{d}_i^k = \tilde{d}_i - d_k$ ;
- 8     decompose  $V^k = Q^k U^k$ ;
- 9     solve the first  $k$  lines of  $U^k \alpha = -Q^{kT} R^k$ ;
- 10     $\Delta \tilde{d}^k = W^k \alpha$ ;
- 11     $d_{k+1} = \tilde{d}_k + \Delta \tilde{d}_k$ ;
- 12 **end**

---

In algorithm 12 the matrices  $V^k$  and  $W^k$  are constructed from the previous iterations and the known values of  $d_0, \dots, d_k$  and  $\tilde{d}_0, \dots, \tilde{d}_k$ .  $\Delta \tilde{d}^k$  is constructed in the column space of  $W^k$  (line 10). For this reason a least squares problem is solved:

$$\alpha = \underset{\beta \in \mathbb{R}^k}{\operatorname{argmin}} \|V^k \beta + R(d_k)\| \quad (3.13)$$

The least squares problem is solved computing the decomposition of  $V^k$  into an orthogonal matrix  $Q^k \in \mathbb{R}^{k \times k}$  and an upper triangular matrix  $U^k \in \mathbb{R}^{n \times k}$  (line 8). Then  $\alpha$  is computed in line 9.

When building matrices  $V^k$  and  $W^k$  (lines 6-7), it is possible to use information from previous time steps.

Finally, to ensure linear independence of columns in the multi-secant system for Jacobian estimation, a filter can be used [35], in order to drop nearly dependent columns of  $Q^k$  and avoid singularity of the approximated Jacobian.

The above algorithm is usually denominated in FSI interface quasi Newton with inverse Jacobian from a least squares model (**IQN-ILS**) (or Anderson acceleration). There exist other algorithms, like generalized Broyden (IQN-IMVJ) or manifold mapping to solve the problem. A complete description of those methods goes beyond the scope of this work: a description of the most common algorithms can be found in [36], while a comparison of the performances can be found in [37].

### 3.3.3 Convergence criteria

At each time step, the coupling algorithm enforce matching conditions at the wet surface up to a convergence criterion. If not sufficiently met, another iteration within the same time step is performed. The fixed point formulation itself induces a criterion based on the residual itself  $r_{k+1}$ .

A scalar, *absolute convergence criterion* can be defined as in Equation 3.14: it is useful for close to zero values of the coupling quantities, when rounding errors become important:

$$\|r_{k+1}\| \leq \epsilon_{abs} \quad (3.14)$$

A more common *relative convergence criterion*, defined in Equation 3.15 is particularly useful when different quantities (e.g. forces and displacements) are compared together to evaluate convergence:

$$\frac{\|r_{k+1}\|}{\|\tilde{d}_{k+1}\|} \leq \epsilon_{rel} \quad (3.15)$$

## 3.4 Interface Mesh and Data Mapping

FSI methods can also be classified considering how the fluid and solid meshes are treated. The *conforming mesh methods* consider the interface as a physical boundary condition (see Section 3.4.2), while *non-conforming mesh methods* treat the boundary location as a constraint imposed on the model equations (see Section 3.4.1) [17].

### 3.4.1 Non-conforming Mesh methods

In non-conforming mesh strategies all interface conditions are imposed as constraints on the flow and structural governing equations. It is possible to use non-conforming meshes for fluid and solid domains as they remain geometrically independent from each other (see Figure 3.5).

This approach is mostly used in *immersed boundary* methods [38]. Coupling is imposed by means of additional force terms appearing in the model equations of the fluid, which impose the kinematic and dynamic conditions. The forces represent the effects of a boundary or body being immersed in the fluid domain. A purely Eulerian mesh (see Section 2.1.1) can be used for the whole computational domain, since the force terms are dynamically added at specific locations to represent the structure.

The fluid forces applied on the solid at the wet surface are computed and used as input for the structural solver, which employs a standard Lagrangian mesh (see Section 2.1.2).

Immersed boundary methods are particularly innovative and are useful to overcome some issues in CFD computations, on the other hand most of the current implementations of FSI problem implement a conforming mesh strategy.

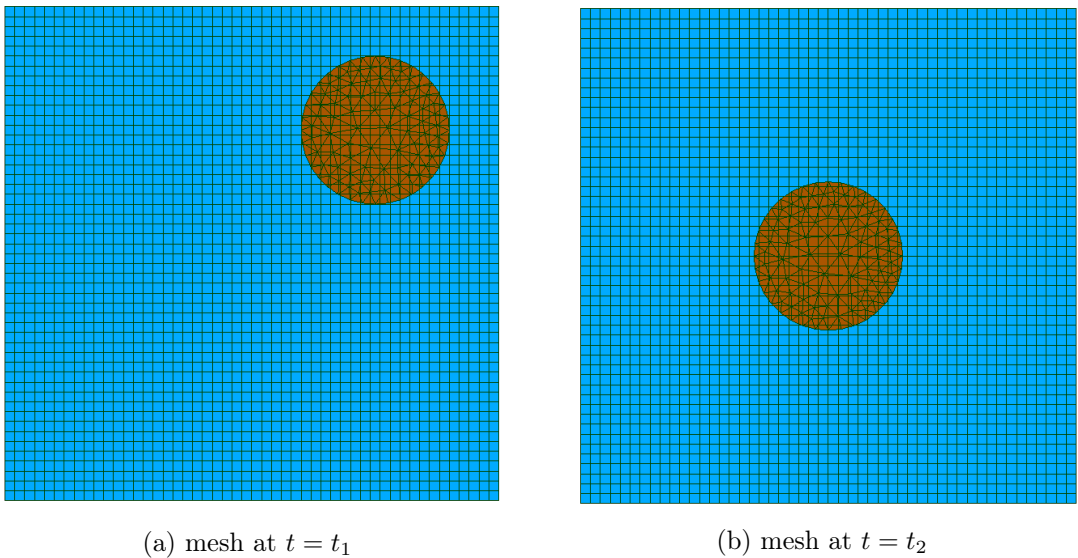


Figure 3.5. non conforming mesh example

### 3.4.2 Conforming Mesh methods

Conforming mesh methods adapt very well to the partitioned approach described in Section 3.1 as they usually consists in the computational steps described above, namely: computation in the fluid, computation in the solid, enforcing of interface condition and mesh movement (see Figure 3.6).

Fluid and structure meshes need share the boundary of the wet surface, as the coupling conditions are enforced by applying kinematic or dynamic conditions to those boundaries. Node-to-node matching of fluid and structure meshes at the interface is not required, as long as a suitable mapping between the interface nodes is performed (see Section 3.4.3).

The match between the interfaces must hold at each time step: this implies that both solid and fluid domains need to deform. Deformation is easily expressed in the solid domain as the structural mesh is usually represented in Lagrangian perspective (see Section 2.1.2). ALE perspective (Section 2.1.3) for the fluid domain becomes necessary in this case.

Mesh deformation can turn out to be a complicated task as in general the fluid mesh is deformed during motion (see Figure 2.4). Mesh smoothing techniques need to be applied in order to keep a good mesh quality in terms of distorted elements which can lead to accuracy loss in simulations. (the following video shows high distorted fluid elements during FSI motion: [video](#)).

Mesh smoothing is generally applied to keep the fluid mesh as uniform and undistorted as possible during movement. There is a wide variety of mesh updating procedures [39]. The *torsional spring analogy* [40] is a fairly simple technique that computes mesh movement considering mesh edges as springs and solving the subsequent Laplace equation that derives from the mesh movement.

Some other references about mesh motion alternatives can be found in [41].

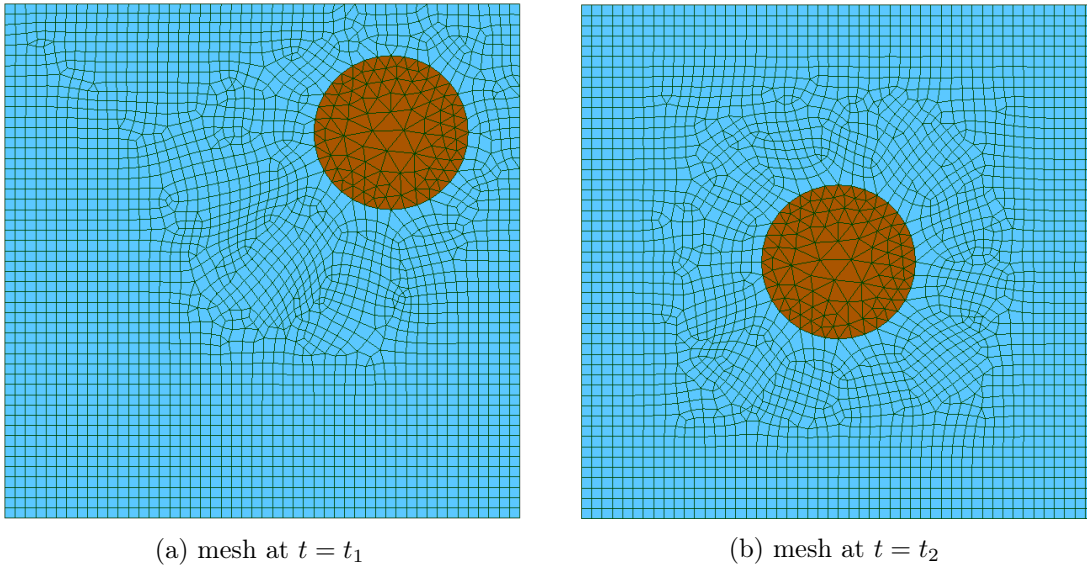


Figure 3.6. conforming mesh example

### 3.4.3 Data Mapping

When partitioned coupling is involved and the meshes are conforming but not node-to-node coincident, the challenge is to correctly map the data between the solid and the fluid sides.

This is a common situation as fluid and solid require a different mesh refinement at the interface.

The mapping procedure needs not only to find the closest available mesh point (or points) on the opposite mesh, but also to preserve mass and energy balance. Variables are basically mapped in two ways: *consistent* and *conservative* forms.

In the *consistent mapping* a value on a node of one grid has the same value of the corresponding node on another grid: that is, it reproduces the values on both meshes. In the *conservative form*, integral values are preserved between meshes. In an FSI problem, nodal forces are mapped in conservative form, while velocities or displacements are mapped in consistent form. An example is shown in Figure 3.7.

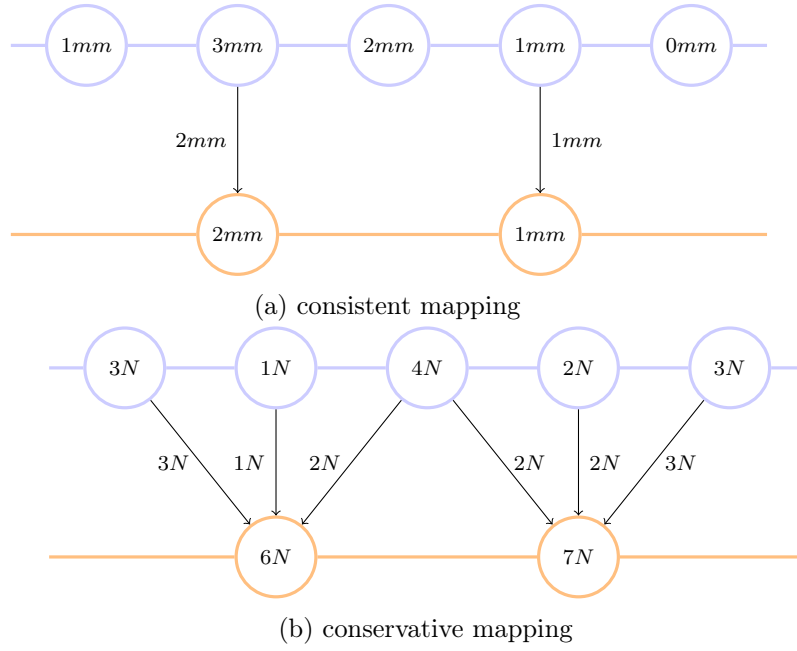


Figure 3.7. Examples of mapping data between non-coincident meshes: consistent (a) and conservative (b) schemes.

different mapping strategies can be implemented [42]:

- *Nearest Neighbor*: finds the closest point on the source mesh and uses its value for the target mesh. It does not require any topological information and is first-order accurate. It is the computationally easiest implementation and it is useful when interface meshes are coincident.
- *Nearest Projection*: projects the points of the target mesh on the source mesh, interpolates the data linearly and assigns the values to the target mesh. It requires topology information for the source mesh. The interpolation on the mesh elements is second order accurate.
- *Radial Basis Function (RBF)*: this method does not requires topological information and works well on general meshes. The mapping uses radial basis functions centered at the grid points of the source mesh [43].

## 3.5 Stability: Added Mass Effect

When a solid moves or vibrates in a fluid domain, the interaction changes the way in which the structure behaves. There exist a vast variety of literature (e.g.: [44], [45], [46], [47]) describing the effects of FSI in terms of *added mass*, *added damping* or even *added stiffness* on a vibrating structure in function of fluid properties (e.g. density or viscosity), or flow properties (e.g. velocity), or geometry.

Besides the physical aspects of the interaction, some numerical issues arise when trying to simulate this kind of problems.

The numerical issue named **AME** is introduced here, as it is relevant for both strongly and weakly coupled partitioned approaches in the solution of FSI problems.

Weakly coupled algorithms give good results in aeroelasticity studies, but they are known to become unstable under certain conditions, in particular when fluid and structure densities are comparable ( $M \approx 1$ , see Section 2.3.4) and when the structure is particularly slender [48]. Under the same conditions, strongly coupled algorithms exhibit convergence problems.

For this reason, the mass ratio  $M$  is a suitable indicator to determine the kind of interaction between solid and fluid: when  $M \ll 1$  (i.e. when the solid is much denser than the fluid), the interaction is weak, while when densities are comparable the interaction is strong and imposes some limits on the partitioned solution techniques.

The problem has been analyzed in literature by means of "toy FSI models" (in [48], [49] or [28]). Even though the number of parameters affecting stability is big and not completely understood in complex scenarios, all of the studies point out the mass-ratio  $M$  as the most relevant parameter.

A simplistic explanation of the phenomenon stems from the idea that at the interface, fluid and structure have no gaps (Section 2.2.4). For this reason, if the structure moves, also the fluid particles around it have to move: the acceleration of the surrounding fluid results in more inertial forces and the structure appears more inert.

Added mass effect appears both in incompressible and in compressible fluid models, but with slightly different effects and implications.

### 3.5.1 AME in compressible regime

In compressible regime, using a weakly coupled algorithm which doesn't enforce mass and energy balance at the interface (see Section 3.2.1) imposes a limit to the mass ratio above which the simulation becomes unstable and the algorithm fails to find a solution [50].

A strongly coupled algorithm (Section 3.2.2) does not become unstable, but converges slowly: many subiterations are needed at each time step in order to reach the required convergence criteria (Section 3.3.3).

It can be shown that, in the compressible case, changing the time step of the partitioned simulation can be beneficial to the solution. The time step reduction to an arbitrarily small value cannot stabilize a weakly coupled algorithms when the stability criterion on the mass ratio is not met, but has an effect on strongly coupled ones [29].

A step size reduction can compensate a higher mass-ratio value [51]: the convergence of a strongly coupled algorithm improves proportionally to the time step reduction. At the theoretical limit of vanishing time step, the monolithic solution could be found.

### 3.5.2 AME in incompressible regime

AME is a much greater issue in incompressible regime than in compressible flows. A simple physical explanation of this fact could be as follows: a deformation of the structure results



in a perturbation of the fluid domain close to the structure, which then propagates through the rest of the fluid domain. In compressible models, the speed at which a perturbation propagates (speed of sound) has a finite value. For this reason the effect of a perturbation is spatially limited during a time step. In contrast, in an incompressible model, the speed at which the aforementioned perturbation propagates through the domain is infinitely large. A change in the geometry affects the whole domain without delay and impacts the whole domain at each time step [48].

It has been observed that loose coupling of fluid and structural part in the context of incompressible flow and slender structures frequently yields unstable computations [51]. However, strict stability limits exist also for strongly coupled algorithms. Those limits have a different relation to the time step with respect to compressible models.

Simulations show that reducing of the time step may result in an increased instability. The AME is inherent in the coupling itself: in sequentially staggered schemes the fluid forces depend upon predicted structural interface displacements rather than the correct ones and thus contain a portion of incorrect coupling forces. This contribution yields the instability [49].

Provided that the stability limit is not exceeded, implicit methods behave differently in incompressible regime: the number of subiterations required to reach convergence during a single time step increases when the time step decreases. Besides, achieving the monolithic solution limit is not guaranteed ([51], [29]).

These observations are consistent with the aforementioned physical explanation.



# Chapter 4

## Software Packages used in this work

This chapter illustrates the main software tools used in this work. First, the coupling library *preCICE* is introduced in Section 4.1. Then, the multibody dynamics solver *MBDyn* being connected to *preCICE* is shortly presented in Section 4.2.

### 4.1 preCICE

The main information concerning *preCICE* is taken from the official documentation: that is [52] and [42]. The *preCICE* website is also a source of documentation<sup>1</sup>.

The open-source<sup>2</sup> software library *preCICE* provides the components to connect traditional single-physics solvers and create a partitioned multi-physics simulation (e.g. fluid-structure interaction, conjugated heat transfer, solid-solid interaction, etc.). It aims at coupling existing solvers in a partitioned black-box manner (see Section 3.2): only minimal information about the solver is available and connection involves just interface nodes. In order to be flexible and easily implemented, the impact on the solvers should be as minimal as possible: for this reason, *preCICE* offers a high level application programming interface (API) (Section 4.1.5) different languages, such as C/C++, Fortran and Python. The ability to switch among different solvers is advantageous as it provides a lot of flexibility in developing and testing new coupled components.

In a nutshell, *preCICE* simply affects the input and observes the output of the solvers (called *participants*). The required data and control elements are accessed using an *adapter*, i.e. a "glue code" that is attached to the corresponding solver and communicates the information with the library.

*preCICE* performs all the actions required to perform a coupled simulation: implements the coupling strategy and convergence criteria (Section 4.1.1), the communication between the participants (Section 4.1.2), the mapping of data between meshes (Section 4.1.3). *preCICE* is configured by means of an extensible markup language (XML) file (Section 4.1.4).

#### 4.1.1 Implemented coupling strategies

Because *preCICE* treats the individual solvers as "black boxes", this information is not available. What is available, however, is the history of the coupling iterations. This can be used to compute an approximate Jacobian and therefore solve Equation 2.10. using a quasi-Newton step. Two variants of this method are offered in *preCICE*: the classical

---

<sup>1</sup>[www.precice.org](http://www.precice.org)

<sup>2</sup>The code can be accessed via Github: [github.com/precice/precice](https://github.com/precice/precice)

interface quasi-Newton (IQN-ILS) and the multi-vector quasi-Newton (IQN-IMVJ). The reader can find more information about these methods in the presentation article of preCICE [6.]. A comparison between them has been published by Lindner et al. [11.]. In the preCICE-terminology, this additional step for improving the stability and accelerating the convergence is called “post-processing”. To summarize, preCICE offers four coupling schemes: serial-explicit, parallel-explicit, serial-implicit, and parallel-implicit. The serial schemes execute the solvers sequentially (the one solver after the other, irrelevant of their internal parallelization) and the second solver uses the updated information from the first one. The parallel schemes execute the solvers in parallel, without updating their input before both solvers complete. In an explicit scheme, the solvers only exchange information once or a fixed number of times. This is simple and fast, but also unstable. An implicit scheme modifies the result of the fixed-point iteration, by solving a fixed-point equation until convergence, either with an under-relaxation or with a more sophisticated quasi-Newton method. In the preCICE terminology, this is called “post-processing” and, together with “checkpointing” are important in an implicit coupling scheme. Please note that, although we refer here to two solvers, preCICE is also capable of coupling multiple solvers at the same time.

preCICE allows both for usage of explicit and implicit coupling techniques. See Section 3.2 to recapitulate the main differences of these approaches. Also, serial and parallel algorithms have been implemented, as well as elaborate procedures particularly suited for black-box coupling. Concerning notation, for all algorithms explained in this section  $n$  denotes the current time step of the computation,  $F_n$  and  $S_n$  are operators representing the fluid and solid solver computation at time instance  $n$ , respectively. They yield the particular fluid and solid solutions  $f_{n+1}$  and  $s_{n+1}$  at time instance  $n + 1$ .

#### Explicit, Serial Algorithm

A serial, weakly coupled algorithm implemented in preCICE is the conventional serial staggered (CSS) procedure ([18]). The algorithm is graphically depicted in Figure 4.3. The fluid solver uses the solid solution at the last time step to compute its current solution (explicit). In contrast, the solid solver needs the current flow solution to compute the structure solution at the same time instance (implicit). Because of this dependency, fluid and structural solvers are said to be executed in a serial, staggered way as they cannot run in parallel and their succession is strictly alternating ([12]).

#### Explicit, Parallel Algorithm

The conventional parallel staggered (CPS) algorithm is similar to the CSS procedure, but allows for parallel execution of both fluid and structure solvers and represents a parallel, explicit coupling algorithm implemented in preCICE ([18]). No implicit dependency as in the case of CSS is present. The succession of this algorithm is shown in Figure 4.4. Fluid and solid solver advance in parallel and exchange coupling data at the end of the time step. However, a drawback compared to the CSS algorithm is the loss of implicitly involving the two solvers, which yields a less stable procedure. Since fluid and solid solvers have to exchange coupling data after each iteration, the overall computation time of the scheme is dependent on the most time-consuming solver, which makes an efficient distribution of computational effort between flow and structure solvers crucial ([12], [18]).

#### Implicit, Serial Strategies

In the following only one time step is discussed, unless stated otherwise. Therefore, all superscripts indicating the time step are neglected. However, subscripts are used to denote subiterations within one time instance. Several implicit algorithms are implemented in preCICE including a Block Gauss-Seidel method with either constant or dynamic Aitken under-relaxation (see Algorithm 1). The Block Gauss-Seidel method is basically an implicit extension of the CSS procedure employing a fixed-point iteration of the form: First of all, the fluid solver runs using the old structural solution. Afterwards, the updated fluid solution

is used by the solid solver to compute the new structure solution. Note that  $sk+1$  is used to indicate that the structural solution is solely obtained by the respective solvers without any modification like e.g. relaxation, while  $sk+1$  indicates that such postprocessing has been applied to the solution. The fixed-point formulation allows to define a residual as shown in Equation 4.2, which can be used to obtain a scalar, absolute convergence criterion (see Equation 4.3), useful for close to zero values of the coupling quantities, when rounding errors become important: track of convergence between two subsequent subiterations: updated solution of the fluid solver, thus not allowing for parallel execution of the single-physics solvers. Since the fluid solver needs a value of the structural solution as input, which is not available for the first iteration of a time step, a predictive value  $sp$  (Line 1, Algorithm 1) is used. The convergence criterion mentioned in Line 3 can be understood as a combination of the absolute and relative limits defined in Equations 4.3 and 4.4. Relaxation techniques as mentioned in Line 6 are used to stabilize the subiteration method. For the case of constant under-relaxation, the relaxed value of the kinematic coupling data is computed as a combination of the old, relaxed and the new, unrelaxed value: with  $0 < ! < 1$ . Roughly speaking, values of  $!$  close to 1 have little stabilizing effect, but result in fast convergence (assuming the method is stable and convergent), whereas for values close to 0 the stabilization is strong, yet convergence is slow and this leads to high computational effort as more subiteration steps are necessary. Consequently, the value should be chosen such that the subiteration process is stable and moreover, converges as fast as possible. Therefore, the choice of  $!$  can be difficult in practice. In contrast to constant under-relaxation, where the relaxation factor  $!$  is fixed, dynamic Aitken relaxation allows for a new factor to be computed in each subiteration. Basically, the dynamic factor is computed from the last two subiteration solutions via linear extrapolation in order to find the solution of the fixed-point system with zero residual, analogous to a root-finding problem with the secant method. The algorithm for obtaining the dynamic Aitken factor is not further described here, as it exceeds the scope of this thesis. Refer to [18], [21] and [25] for details.

Procedures Predestinated for Black-Box Coupling As coupling of black-box solvers is one of the major issues of preCICE, no Newton methods can be used for implicit coupling, since they require interface Jacobian information, which is typically not accessible for this kind of solvers. Therefore, algorithms which make use of approximations of the Jacobian are of importance. Two variants of these are implemented in preCICE, for serial and parallel usage. The serial algorithm is called IQN-ILS, which stands for Interface Quasi-Newton with Approximation of the Inverse of the Interface Jacobian Matrix by Least-Squares. In a sequential manner, fluid and structural solvers are executed, followed by the IQN-ILS algorithm, which modifies the structural solution such that the underlying fixed-point iteration converges. This solution is then fed back to the fluid solver and the computation circle starts over, as long as the fixed-point is not yet reached up to a specified convergence criterion. The parallel procedure is named V-IQN, originating from a vectorial fixed-point formulation of the problem (displacements and forces are gathered in a single vector). Again the procedure is based on an Interface Quasi-Newton approach. The method allows for fluid and solid solver to be run simultaneously, before the V-IQN algorithm modifies the vector of displacements and forces such that the fixed-point iteration converges. If the convergence limit is not yet reached after a subiteration, these modified values are used as input for the next iteration of fluid and structure solvers, respectively. I do not explain these elaborate methods further. Refer to [8] for the IQN-ILS method and to [40] and [27] for the V-IQN algorithm.

#### 4.1.2

### 4.1.2 Communication strategies

The individual participants need to communicate with each other, in order to exchange information. The participants may be executed in multiple processes, possibly running on different nodes of a supercomputing system. The simulation software may not use MPI and may not be open-source. However, these are no obstacles for preCICE, since it allows for communication using either MPI ports (MPI 2.0), or TCP/IP sockets (implemented with Boost.Asio3 .), which are lower-level and allow to couple closed-source software as well. In each parallel solver, one “master” process is chosen to manage the steering of the simulation. However, no central instance (“server”) is required in preCICE. The participating processes use asynchronous point-to-point (M:N) communication. The communication channels are static and set in the beginning of the coupled simulation. This currently poses limitations in using preCICE with dynamically adaptive meshes or immersed boundaries, limitations that are going to be surpassed in future releases [6., 16.].

Interfield parallelism is an important topic when it comes to high-performance computing (HPC) on massively parallel systems. But the execution time of the solver processes does not solely determine overall runtimes of simulations. A high level of parallelization also induces the necessity of efficient forms of communication between the distributed processes so that data transfer does not become a dominant bottleneck. preCICE offers three different means of communication based on files, sockets and message passing interface (MPI) ([18]). A fully parallel process-to-process communication approach (both via sockets and MPI) for preCICE is implemented in [37]. File communication is a very basic form of communication. Solver processes write data to and read data from files, which are stored on the hard drive of a computer. Communication is limited to a one-to-one fashion, meaning that a single writer and a single reader communicate with each other. Each file is named uniquely in order to identify the writer and reader by their respective names. Furthermore, the file name contains a message counting number. In order to avoid writer and reader processing the same file simultaneously, the currently working process renames the file and hides it by that manner from the communication partner. Reading is implemented such that busy waiting is used to check for the correctly named file. This is a drawback of file communication as it blocks computational resources. Moreover, due to the inherent latency of the hard drive, the technique is not feasible for frequent data exchange. It is implemented in preCICE solely for testing purposes as it allows to easily trace back errors ([18]). MPI ([16]) is typically used for parallelizing applications (intrafield parallelism) in a way that parallel processes run the same code, differing by the MPI rank/index3. However, in preCICE, MPI communication is used to exchange data between processes of different applications, namely the instances of the single-physics solvers. A big advantage of this communication method is that MPI is available on most scientific computers and offers qualities, which are relevant in the field of HPC, such as high data throughput and small latency. In preCICE, MPI communication can be set up either via a single communication space containing all executables (which are then subgrouped for the individual solvers) or via different spaces. This means of communication can be quite prone to incompatibilities of software with different implemented versions of MPI. Therefore, it may be necessary to adapt/change the underlying MPI versions of the respective single-physics solvers or of preCICE. Especially in the case of closed-source solvers, this adaption might not be possible and thus communication via MPI might have to be discarded. Communication is performed asynchronously (non-blocking), which is highly relevant for fully parallel process-to-process communication ([37], [18]). Sockets preCICE also supports communication via Transmission Control Protocol/Internet Protocol (TCP/IP) sockets. Although their usage is rather unconventional in HPC, they are used in preCICE as they are a very elaborate, well-known means of network communication and therefore,

mostly bug-free. Furthermore, unlike in the case of MPI, different TCP/IP socket versions for different solvers to be coupled do usually not yield runtime incompatibilities. Again, the communication procedure is asynchronous (non-blocking) ([37]). Gatzhammer shows in [18] that, indeed, MPI is the best-performing communication technique implemented in preCICE as it outperforms socket- and file-based communication especially for use cases of data exchange with higher numbers of nodes<sup>4</sup>. However, socket communication follows closely, such that both techniques are very well-suited for larger-scale simulations.

### 4.1.3 Data mapping

A challenge in partitioned coupling is to map the required data between non-conforming meshes. The mapper not only needs to find the closest available mesh point, but also to not disrupt the mass and energy balances. Therefore, preCICE maps variables between meshes either in a consistent or in a conservative form. In the consistent mapping, the value of a node at the one grid is the same as the value of the corresponding node at the other grid. The consistent form simply reproduces the values from the one mesh to the other. The conservative form, on the other hand, makes sure that the integral values are preserved. For example, forces are mapped in a conservative fashion, since the sum of forces on both sides of an interface needs to be the same. On the contrary, fields such as temperatures or velocities are mapped consistently. An example is shown in Figure 2.3.. The following mapping methods are implemented in preCICE [6.] (in their consistent variant): • Nearest neighbor: Finds the closest point on the source mesh and uses its value. It does not require any topological information and is first-order accurate. • Nearest projection: Projects the target mesh points on the mesh elements of the source mesh, performs linear interpolation on them and assigns the interpolated values back on the target mesh. Because of the usually small distance between two meshes (normal to the interface), in relation to the size of the elements, this method is second-order accurate. • Radial Basis Function: Requires no topological information, and it does not search or project any points. It constructs an interpolant on the source mesh, using radial basis functions centered at the grid points and evaluates it on the target mesh. preCICE offers a wide variety of basis functions, but Gaussian and thin plate splines are the most widely used. A cut-off radius bounds the support of these functions and allows to keep the communication in a parallel environment local. In preCICE, the RBF mapping uses the PETSc library<sup>2</sup>. [2., 16.]. All the respective conservative mapping methods are also available

In FSI simulations, fluid and structure meshes do not necessarily coincide in a node-to-node manner at the wet surface. In fact, typically fluid and structural domains are spatially discretized to different levels of refinement. In most cases, fluid meshes are finer than solid grids, meaning that at the wet surface more fluid than structural nodes appear. This situation is sketched in Figure 4.5. Therefore, when coupling data needs to be exchanged at the wet surface, some mapping between fluid and solid nodes must be applied in order to be able to interpolate data between them. preCICE offers three different methods for this, namely nearest-neighbor (NN) and nearest-projection (NP) mapping, as well as an interpolation method based on radial basis functions (RBF) ([18]). For all implemented procedures in preCICE, mapping can be applied in either consistent or conservative fashion, which must be chosen dependent on what quantities are exchanged at the wet surface (e.g. forces or stresses, displacements or velocities) ([18]). As is the case for the coupling described in this thesis (and most of the numerical testcases, which are shown), a fine fluid mesh and a coarse solid mesh meet at their common interface (as depicted in Figure 4.5). Forces need to be mapped from fluid to corresponding structural nodes and displacements in reverse from solid to fluid nodes. As the number of fluid nodes exceeds that of the structure, in general a single solid

node is assigned to several fluid nodes<sup>5</sup>. If forces are mapped from these multiple fluid nodes to the solid node, all of the assigned fluid nodes contribute to the overall force value at the structural node in an additive manner. Such a mapping is called conservative, as the overall sum of the forces on both fluid and structure side at the wet surface remains constant, i.e. it is conserved. In contrast, when displacements are mapped from a single solid node to the fluid nodes, it is not useful to distribute the single displacement value among the fluid nodes such that the displacements of the fluid nodes sum up to the displacement of the solid node. Rather, all fluid nodes assigned to that single solid node experience the same displacement. Such a mapping is called consistent, as the mapped value is transferred exactly ([18], [7]). A schematic example of conservative and consistent interpolation is depicted in Figure 4.6 for the NN method. Conservative mapping of forces and consistent mapping of displacements is used in the coupling procedure performed in this thesis.

Nearest-Neighbor NN mapping is the most basic method available in preCICE. Each node at the wet surface of a mesh searches for the corresponding closest neighboring node of the other mesh. In this context, "closest" is to be interpreted in the sense of the shortest Euclidean distance ([6]). Of course, this allows for multiple nodes of a fine mesh to be assigned to a single node of a coarse mesh as mentioned before. For this kind of mapping, preCICE needs no information regarding mesh connections and elements, the sole position of the nodes at the wet surface is sufficient ([18]).

Nearest-Projection In the case of NP mapping, the shortest distance of a node of one mesh to the other mesh is detected. For a general three-dimensional case, when the interface between fluid and solid is a surface, a node's shortest distance to the other mesh may occur at either a node, an edge or a surface element of the partner mesh. Thus, for each node, preCICE computes the distance to the NN, the nearest edge and the nearest surface element ([18]). For a graphical representation of this situation, see Figure 4.7. Consequently, the shortest distance is chosen among those three, which determines whether one node (node is nearest), two nodes mapping. If the shortest distance occurs at an edge or a surface element, in general, not all nodes of the respective edge or surface element have the same influence on the assigned node of the partner mesh. Depending on how close these nodes are to the projected one, weights are calculated, which describe the differently strong influence. As for this method preCICE needs to know not only about the positions of all interface nodes, but also mesh connections in order to recognize edges and elements, at least one full mesh representation must be fed to preCICE during startup of a simulation ([18]). Radial Basis Functions Interpolation with RBF can be done with either compactly or globally supported functions. This means that the spatial influence of nodes, from which data is to be mapped, is either limited to a certain Euclidean range, the support radius  $r$ , or not. In the latter case, each node at the wet surface of one mesh influences each node at the interface of the other mesh. In contrast, with compactly supported RBF, only those nodes of the partnering mesh are influenced, which are located within a sphere around a node of the first mesh with radius equal to the support radius. In both cases the exact strength of the influence (and its dependency on distance between two nodes) is then determined by the RBF itself:

where  $k_{xk}$  denotes the Euclidean distance between a node of the first and the second mesh. Moreover, Generally, the wider the support of a basis function is, the better is the approximation. Yet the computation of the interpolation requires more effort as influences of a lot of nodes have to be taken into account. In reverse, a narrow support yields an interpolation system, which is easy to solve, but the approximation might suffer from it resulting in larger mapping errors. Choosing an adequate support radius is, therefore, a difficult task in practice. Moreover, the support radius should be kept fixed for all wet surface nodes of a mesh as varying from node to node might not lead to an interpolation solution ([1], [33]). Several different RBF are available in preCICE<sup>7</sup>. Globally supported functions



include a thin-plate spline, (inverse) multiquadrics, a volume spline and a Gaussian, while the following compactly supported RBF are implemented: A thin-plate spline of continuity C2, as well as polynomials of continuity C0 and C6, respectively ([18]).

#### 4.1.4 Configuration

In order to start a multi-physics simulation with preCICE, all the participating, adapted solvers are started normally, in arbitrary order. Two configuration files are expected: • Adapter’s configuration file: Normally this is a YAML file and contains information about the boundaries that are used for the coupling, the kinds of exchanged data, the name of the used mesh and the name of the common preCICE configuration file. It may also contain other parameters, special to each adapter. • preCICE configuration file: This is an XML file and it is shared among all the participants. It defines the coupling interfaces between the participating solvers, the meshes over which coupling data is exchanged, the kinds of exchanged data, the way these data are mapped from the one mesh to the other and it provides all the necessary options for the respective coupling scheme. The OpenFOAM adapter’s configuration file is described in Section 5.4.. For the configuration of preCICE, the reader is referred to the wiki of preCICE for the latest information and detailed tutorials<sup>4</sup>

#### 4.1.5 Application Program Interface

Each participating solver needs to be modified to link to the preCICE library and call methods from its application programming interface. Usually, the calls to the API are grouped together in a preCICE adapter. While preCICE is written in C++, it provides an API also for C, Fortran and Python. An excerpt from the C++ API is shown in Listing 2.1., as drawn from the preCICE source code documentation<sup>5</sup> .. A coupling consists of a configuration and an initialization phase, multiple coupling advancements and a finalization phase. First, a SolverInterface object needs to be created. The constructor expects the rank of the process and the size of the communicator in the parallel execution environment. The configure() method sets the name of the preCICE configuration file, reads and validates it and sets up the communication inside the solver. The methods that follow in Listing 2.1. are called “steering methods”. The initialize() method sets up the data structures and communication channels to other participants. Here the first communication happens, as the participants exchange meshes and, if necessary, re-partition them. It returns the maximum time step size that the solver is allowed to execute next. It is followed by the initializeData(), which is optional and transfers any initial non-zero coupling data values among participants. The equation coupling, the data mapping and the communication are all hidden inside the advance() method. This method also returns the maximum time step size allowed. The last method to call is finalize(), which destroys the data structures and closes the communication channels. The solvers need to define their interface meshes. Only some of the methods for mesh definition are listed in Listing 2.1.. Each mesh and each node on the mesh are assigned an integer ID. The getMeshID() gets the ID of the mesh over which the coupling data of the specific kind are exchanged. The setMeshVertex() creates a vertex on the specified mesh and position and returns the id of the vertex. For performance reasons, multiple vertices can be defined at once with setMeshVertices(). Additionally, topological information, such as edges or triangles can be passed to preCICE with additional methods which are not listed here. After defining the meshes, they need to be assigned data values. This is done by methods with names write\*Data(), which fill the “buffers” with data from the solver’s mesh or with methods read\*Data(), which read data from the buffers into the solver’s mesh. Since preCICE distinguishes between scalar and vector data, both kinds of methods are

available. Again, for performance reasons, blocks of data can be processed together using the respective `writeBlock*Data()` and `readBlock*Data()`. Please note that these data are not communicated among participants before the next `advance()` (or `initializeData()`). A number of auxiliary methods allow to access information important for the coupling, such as whether the coupled simulation is still running, if writing or reading data is expected or if the current coupling time step has finished successfully. The solver can also inquire if it is required to execute a specific action (e.g. to write or to read a checkpoint) and it can inform preCICE that it fulfilled these tasks [16.]. An example of an adapted solver is shown in Listing 2.2., as published in the presentation article of preCICE [6.]. A more detailed example is presented in the wiki of preCICE6 ..

..

### 4.1.6 Official Adapters

This thesis presents an OpenFOAM adapter for preCICE. It is based on previous work and it considers other available adapters for specific solvers that use or are part of OpenFOAM or foam-extend. These adapters are described in Chapter 4.. OpenFOAM is only one of the simulation software packages that preCICE supports. Official adapters are currently available for several other free solvers, including CalculiX, Code-Aster and SU2 [17.]. Closed-source software is also supported, including COMSOL and Fluent. The adapters are available in their own repositories, under the umbrella of the preCICE organization on GitHub7 .. A detailed list, including several third-party adapters, can be found in the website of preCICE8 .. Adapting an in-house solver is also possible and more, unpublished adapters are known to exist [5.]. 6preCICE

[53] Official adapters

## 4.2 MBDyn

## Chapter 5

# MBDyn Adapter and its integration

Lorem ipsum dolor sit amet, consectetur adipiscing elit, sed eiusmod tempor incididunt ut labore et dolore magna aliqua. Ut enim ad minim veniam, quis nostrum exercitationem ullam corporis suscipit laboriosam, nisi ut aliquid ex ea commodi consequatur. Quis aute iure reprehenderit in voluptate velit esse cillum dolore eu fugiat nulla pariatur.



# Chapter 6

## Validation Test-cases

Lorem ipsum dolor sit amet, consectetur adipiscing elit, sed eiusmod tempor incididunt ut labore et dolore magna aliqua. Ut enim ad minim veniam, quis nostrum exercitationem ullam corporis suscipit laboriosam, nisi ut aliquid ex ea commodi consequatur. Quis aute iure reprehenderit in voluptate velit esse cillum dolore eu fugiat nulla pariatur.



## Conclusions

41

1.  $\frac{1}{2}$       2.  $\frac{1}{3}$       3.  $\frac{1}{4}$       4.  $\frac{1}{5}$       5.  $\frac{1}{6}$       6.  $\frac{1}{7}$       7.  $\frac{1}{8}$       8.  $\frac{1}{9}$       9.  $\frac{1}{10}$       10.  $\frac{1}{11}$       11.  $\frac{1}{12}$       12.  $\frac{1}{13}$       13.  $\frac{1}{14}$       14.  $\frac{1}{15}$       15.  $\frac{1}{16}$       16.  $\frac{1}{17}$       17.  $\frac{1}{18}$       18.  $\frac{1}{19}$       19.  $\frac{1}{20}$       20.  $\frac{1}{21}$       21.  $\frac{1}{22}$       22.  $\frac{1}{23}$       23.  $\frac{1}{24}$       24.  $\frac{1}{25}$       25.  $\frac{1}{26}$       26.  $\frac{1}{27}$       27.  $\frac{1}{28}$       28.  $\frac{1}{29}$       29.  $\frac{1}{30}$       30.  $\frac{1}{31}$       31.  $\frac{1}{32}$       32.  $\frac{1}{33}$       33.  $\frac{1}{34}$       34.  $\frac{1}{35}$       35.  $\frac{1}{36}$       36.  $\frac{1}{37}$       37.  $\frac{1}{38}$       38.  $\frac{1}{39}$       39.  $\frac{1}{40}$       40.  $\frac{1}{41}$       41.  $\frac{1}{42}$       42.  $\frac{1}{43}$       43.  $\frac{1}{44}$       44.  $\frac{1}{45}$       45.  $\frac{1}{46}$       46.  $\frac{1}{47}$       47.  $\frac{1}{48}$       48.  $\frac{1}{49}$       49.  $\frac{1}{50}$       50.  $\frac{1}{51}$       51.  $\frac{1}{52}$       52.  $\frac{1}{53}$       53.  $\frac{1}{54}$       54.  $\frac{1}{55}$       55.  $\frac{1}{56}$       56.  $\frac{1}{57}$       57.  $\frac{1}{58}$       58.  $\frac{1}{59}$       59.  $\frac{1}{60}$       60.  $\frac{1}{61}$       61.  $\frac{1}{62}$       62.  $\frac{1}{63}$       63.  $\frac{1}{64}$       64.  $\frac{1}{65}$       65.  $\frac{1}{66}$       66.  $\frac{1}{67}$       67.  $\frac{1}{68}$       68.  $\frac{1}{69}$       69.  $\frac{1}{70}$       70.  $\frac{1}{71}$       71.  $\frac{1}{72}$       72.  $\frac{1}{73}$       73.  $\frac{1}{74}$       74.  $\frac{1}{75}$       75.  $\frac{1}{76}$       76.  $\frac{1}{77}$       77.  $\frac{1}{78}$       78.  $\frac{1}{79}$       79.  $\frac{1}{80}$       80.  $\frac{1}{81}$       81.  $\frac{1}{82}$       82.  $\frac{1}{83}$       83.  $\frac{1}{84}$       84.  $\frac{1}{85}$       85.  $\frac{1}{86}$       86.  $\frac{1}{87}$       87.  $\frac{1}{88}$       88.  $\frac{1}{89}$       89.  $\frac{1}{90}$       90.  $\frac{1}{91}$       91.  $\frac{1}{92}$       92.  $\frac{1}{93}$       93.  $\frac{1}{94}$       94.  $\frac{1}{95}$       95.  $\frac{1}{96}$       96.  $\frac{1}{97}$       97.  $\frac{1}{98}$       98.  $\frac{1}{99}$       99.  $\frac{1}{100}$       100.  $\frac{1}{101}$       101.  $\frac{1}{102}$       102.  $\frac{1}{103}$       103.  $\frac{1}{104}$       104.  $\frac{1}{105}$       105.  $\frac{1}{106}$       106.  $\frac{1}{107}$       107.  $\frac{1}{108}$       108.  $\frac{1}{109}$       109.  $\frac{1}{110}$       110.  $\frac{1}{111}$       111.  $\frac{1}{112}$       112.  $\frac{1}{113}$       113.  $\frac{1}{114}$       114.  $\frac{1}{115}$       115.  $\frac{1}{116}$       116.  $\frac{1}{117}$       117.  $\frac{1}{118}$       118.  $\frac{1}{119}$       119.  $\frac{1}{120}$       120.  $\frac{1}{121}$       121.  $\frac{1}{122}$       122.  $\frac{1}{123}$       123.  $\frac{1}{124}$       124.  $\frac{1}{125}$       125.  $\frac{1}{126}$       126.  $\frac{1}{127}$       127.  $\frac{1}{128}$       128.  $\frac{1}{129}$       129.  $\frac{1}{130}$       130.  $\frac{1}{131}$       131.  $\frac{1}{132}$       132.  $\frac{1}{133}$       133.  $\frac{1}{134}$       134.  $\frac{1}{135}$       135.  $\frac{1}{136}$       136.  $\frac{1}{137}$       137.  $\frac{1}{138}$       138.  $\frac{1}{139}$       139.  $\frac{1}{140}$       140.  $\frac{1}{141}$       141.  $\frac{1}{142}$       142.  $\frac{1}{143}$       143.  $\frac{1}{144}$       144.  $\frac{1}{145}$       145.  $\frac{1}{146}$       146.  $\frac{1}{147}$       147.  $\frac{1}{148}$       148.  $\frac{1}{149}$       149.  $\frac{1}{150}$       150.  $\frac{1}{151}$       151.  $\frac{1}{152}$       152.  $\frac{1}{153}$       153.  $\frac{1}{154}$       154.  $\frac{1}{155}$       155.  $\frac{1}{156}$       156.  $\frac{1}{157}$       157.  $\frac{1}{158}$       158.  $\frac{1}{159}$       159.  $\frac{1}{160}$       160.  $\frac{1}{161}$       161.  $\frac{1}{162}$       162.  $\frac{1}{163}$       163.  $\frac{1}{164}$       164.  $\frac{1}{165}$       165.  $\frac{1}{166}$       166.  $\frac{1}{167}$       167.  $\frac{1}{168}$       168.  $\frac{1}{169}$       169.  $\frac{1}{170}$       170.  $\frac{1}{171}$       171.  $\frac{1}{172}$       172.  $\frac{1}{173}$       173.  $\frac{1}{174}$       174.  $\frac{1}{175}$       175.  $\frac{1}{176}$       176.  $\frac{1}{177}$       177.  $\frac{1}{178}$       178.  $\frac{1}{179}$       179.  $\frac{1}{180}$       180.  $\frac{1}{181}$       181.  $\frac{1}{182}$       182.  $\frac{1}{183}$       183.  $\frac{1}{184}$       184.  $\frac{1}{185}$       185.  $\frac{1}{186}$       186.  $\frac{1}{187}$       187.  $\frac{1}{188}$       188.  $\frac{1}{189}$       189.  $\frac{1}{190}$       190.  $\frac{1}{191}$       191.  $\frac{1}{192}$       192.  $\frac{1}{193}$       193.  $\frac{1}{194}$       194.  $\frac{1}{195}$       195.  $\frac{1}{196}$       196.  $\frac{1}{197}$       197.  $\frac{1}{198}$       198.  $\frac{1}{199}$       199.  $\frac{1}{200}$       200.  $\frac{1}{201}$       201.  $\frac{1}{202}$       202.  $\frac{1}{203}$       203.  $\frac{1}{204}$       204.  $\frac{1}{205}$       205.  $\frac{1}{206}$       206.  $\frac{1}{207}$       207.  $\frac{1}{208}$       208.  $\frac{1}{209}$       209.  $\frac{1}{210}$       210.  $\frac{1}{211}$       211.  $\frac{1}{212}$       212.  $\frac{1}{213}$       213.  $\frac{1}{214}$       214.  $\frac{1}{215}$       215.  $\frac{1}{216}$       216.  $\frac$



ut labore et dolore magna aliqua. Ut enim ad minim veniam, quis nostrum exercitationem ullam corporis suscipit laboriosam, nisi ut aliquid ex ea commodi consequatur. Quis aute iure reprehenderit in voluptate velit esse cillum dolore eu fugiat nulla pariatur. Excepteur sint obcaecat cupiditat non proident, sunt in culpa qui officia deserunt mollit anim id est laborum. Lorem ipsum dolor sit amet, consectetur adipisci elit, sed eiusmod tempor incidunt ut labore et dolore magna aliqua. Ut enim ad minim veniam, quis nostrum exercitationem ullam corporis suscipit laboriosam, nisi ut aliquid ex ea commodi consequatur. Quis aute iure reprehenderit in voluptate velit esse cillum dolore eu fugiat nulla pariatur. Excepteur sint obcaecat cupiditat non proident, sunt in culpa qui officia deserunt mollit anim id est laborum. Lorem ipsum dolor sit amet, consectetur adipisci elit, sed eiusmod tempor incidunt ut labore et dolore magna aliqua. Ut enim ad minim veniam, quis nostrum exercitationem ullam corporis suscipit laboriosam, nisi ut aliquid ex ea commodi consequatur. Quis aute iure reprehenderit in voluptate velit esse cillum dolore eu fugiat nulla pariatur. Excepteur sint obcaecat cupiditat non proident, sunt in culpa qui officia deserunt mollit anim id est laborum. Lorem ipsum dolor sit amet, consectetur adipisci elit, sed eiusmod tempor incidunt ut labore et dolore magna aliqua. Ut enim ad minim veniam, quis nostrum exercitationem ullam corporis suscipit laboriosam, nisi ut aliquid ex ea commodi consequatur. Quis aute iure reprehenderit in voluptate velit esse cillum dolore eu fugiat nulla pariatur. Excepteur sint obcaecat cupiditat non proident, sunt in culpa qui officia deserunt mollit anim id est laborum. Lorem ipsum dolor sit amet, consectetur adipisci elit, sed eiusmod tempor incidunt ut labore et dolore magna aliqua. Ut enim ad minim veniam, quis nostrum exercitationem ullam corporis suscipit laboriosam, nisi ut aliquid ex ea commodi consequatur.



# First Appendix

45

[illegible]





ut labore et dolore magna aliqua. Ut enim ad minim veniam, quis nostrum exercitationem ullam corporis suscipit laboriosam, nisi ut aliquid ex ea commodi consequatur. Quis aute iure reprehenderit in voluptate velit esse cillum dolore eu fugiat nulla pariatur. Excepteur sint obcaecat cupiditat non proident, sunt in culpa qui officia deserunt mollit anim id est laborum. Lorem ipsum dolor sit amet, consectetur adipisci elit, sed eiusmod tempor incidunt ut labore et dolore magna aliqua. Ut enim ad minim veniam, quis nostrum exercitationem ullam corporis suscipit laboriosam, nisi ut aliquid ex ea commodi consequatur. Quis aute iure reprehenderit in voluptate velit esse cillum dolore eu fugiat nulla pariatur. Excepteur sint obcaecat cupiditat non proident, sunt in culpa qui officia deserunt mollit anim id est laborum. Lorem ipsum dolor sit amet, consectetur adipisci elit, sed eiusmod tempor incidunt ut labore et dolore magna aliqua. Ut enim ad minim veniam, quis nostrum exercitationem ullam corporis suscipit laboriosam, nisi ut aliquid ex ea commodi consequatur. Quis aute iure reprehenderit in voluptate velit esse cillum dolore eu fugiat nulla pariatur. Excepteur sint obcaecat cupiditat non proident, sunt in culpa qui officia deserunt mollit anim id est laborum. Lorem ipsum dolor sit amet, consectetur adipisci elit, sed eiusmod tempor incidunt ut labore et dolore magna aliqua. Ut enim ad minim veniam, quis nostrum exercitationem ullam corporis suscipit laboriosam, nisi ut aliquid ex ea commodi consequatur.





# Acronyms

<b>FSI</b>	Fluid-Structure Interaction
<b>MBDyn</b>	MultiBody Dynamics analysis software
<b>preCICE</b>	precise Code Interaction Coupling Environment
<b>ALE</b>	arbitrary Lagrangian-Eulerian
<b>CFD</b>	Computational Fluid Dynamics
<b>CSM</b>	Computational Solid Mechanics
<b>NSE</b>	Navier Stokes Equations
<b>PDE</b>	Partial Differential Equations
<b>VWP</b>	Virtual Work Principle
<b>FEM</b>	Finite Element Method
<b>AME</b>	added mass effect
<b>FPI</b>	fixed point iteration
<b>IQN-ILS</b>	interface quasi Newton with inverse Jacobian from a least squares model
<b>RBF</b>	Radial Basis Function
<b>API</b>	application programming interface
<b>XML</b>	extensible markup language



# Bibliography

- [1] G. L. Ghiringhelli, P. Masarati, M. Morandini, and D. Muffo, “Integrated aeroservoelastic analysis of induced strain rotor blades,” *Mechanics of Advanced Materials and Structures*, vol. 15, no. 3-4, pp. 291–306, 2008.
- [2] R. C. Batra, *Elements of continuum mechanics*. Aiaa, 2006.
- [3] J. Cheng, G. Zhao, Z. Jia, Y. Chen, S. Wang, and W. Wen, “Sliding free lagrangian-eulerian finite element method,” in *International Conference on Computational Science*, 2006.
- [4] J. Donea, A. Huerta, J.-P. Ponthot, and A. Rodríguez-Ferran, “Arbitrary lagrangian-eulerian methods,” *Encyclopedia of Computational Mechanics Second Edition*, pp. 1–23, 2017.
- [5] J. T. Xing, “Chapter 3 - fundamentals of continuum mechanics,” in *Fluid-Solid Interaction Dynamics*, J. T. Xing, Ed. Academic Press, 2019, pp. 57 – 101. [Online]. Available: <http://www.sciencedirect.com/science/article/pii/B9780128193525000033>
- [6] S. Lipton, J. A. Evans, Y. Bazilevs, T. Elguedj, and T. J. Hughes, “Robustness of isogeometric structural discretizations under severe mesh distortion,” *Computer Methods in Applied Mechanics and Engineering*, vol. 199, no. 5-8, pp. 357–373, 2010.
- [7] A. Bertram, *Elasticity and plasticity of large deformations*. Springer, 2012.
- [8] A. De Boer, M. Van der Schoot, and H. Bijl, “Mesh deformation based on radial basis function interpolation,” *Computers & structures*, vol. 85, no. 11-14, pp. 784–795, 2007.
- [9] E. Ramm and W. Wall, “Fluid-structure interaction based upon a stabilized (ale) finite element method,” in *4th World Congress on Computational Mechanics: New Trends and Applications*, CIMNE, Barcelona, 1998, pp. 1–20.
- [10] L. Quartapelle and F. Auteri, *Fluidodinamica incompressibile*. Casa editrice ambrosiana, 2013.
- [11] —, *Fluidodinamica comprimibile*. Casa editrice ambrosiana, 2013.
- [12] S. B. Pope, “Turbulent flows,” 2001.
- [13] G. Galdi, *An introduction to the mathematical theory of the Navier-Stokes equations: Steady-state problems*. Springer Science & Business Media, 2011.
- [14] R. W. Ogden, *Non-linear elastic deformations*. Courier Corporation, 1997.
- [15] K. D. Hjelmstad, *Fundamentals of structural mechanics*. Springer Science & Business Media, 2007.

- [16] G. L. Ghiringhelli, P. Masarati, and P. Mantegazza, “Multibody implementation of finite volume c beams,” *AIAA journal*, vol. 38, no. 1, pp. 131–138, 2000.
- [17] G. Hou, J. Wang, and A. Layton, “Numerical methods for fluid-structure interaction—a review,” *Communications in Computational Physics*, vol. 12, no. 2, pp. 337–377, 2012.
- [18] H. Hanche-Olsen, “Buckingham’s pi-theorem,” *NTNU*: <http://www.math.ntnu.no/~hanche/notes/buckingham/buckingham-a4.pdf>, 2004.
- [19] J.-D. Hardtke, “On buckingham’s  $\pi$ -theorem,” *arXiv preprint arXiv:1912.08744*, 2019.
- [20] R. W. Fox, A. T. McDonald, and J. W. Mitchell, *Fox and McDonald’s introduction to fluid mechanics*. John Wiley & Sons, 2011.
- [21] S. Longo, *Analisi Dimensionale e Modellistica Fisica: Principi e applicazioni alle scienze ingegneristiche*. Springer Science & Business Media, 2011.
- [22] E. De Langre, *Fluides et solides*. Editions Ecole Polytechnique, 2001.
- [23] B. Hübner, E. Walhorn, and D. Dinkler, “A monolithic approach to fluid–structure interaction using space–time finite elements,” *Computer methods in applied mechanics and engineering*, vol. 193, no. 23-26, pp. 2087–2104, 2004.
- [24] P. Ryzhakov, R. Rossi, S. Idelsohn, and E. Oñate, “A monolithic lagrangian approach for fluid–structure interaction problems,” *Computational mechanics*, vol. 46, no. 6, pp. 883–899, 2010.
- [25] T. Richter, *Fluid-structure interactions: models, analysis and finite elements*. Springer, 2017, vol. 118.
- [26] J. Degroote, K.-J. Bathe, and J. Vierendeels, “Performance of a new partitioned procedure versus a monolithic procedure in fluid–structure interaction,” *Computers & Structures*, vol. 87, no. 11-12, pp. 793–801, 2009.
- [27] C. Farhat, K. G. Van der Zee, and P. Geuzaine, “Provably second-order time-accurate loosely-coupled solution algorithms for transient nonlinear computational aeroelasticity,” *Computer methods in applied mechanics and engineering*, vol. 195, no. 17-18, pp. 1973–2001, 2006.
- [28] M. Mehl, B. Uekermann, H. Bijl, D. Blom, B. Gatzhammer, and A. Van Zuijlen, “Parallel coupling numerics for partitioned fluid–structure interaction simulations,” *Computers & Mathematics with Applications*, vol. 71, no. 4, pp. 869–891, 2016.
- [29] E. H. van Brummelen, “Added mass effects of compressible and incompressible flows in fluid-structure interaction,” *Journal of Applied mechanics*, vol. 76, no. 2, 2009.
- [30] U. Küttler and W. A. Wall, “Fixed-point fluid–structure interaction solvers with dynamic relaxation,” *Computational mechanics*, vol. 43, no. 1, pp. 61–72, 2008.
- [31] B. M. Irons and R. C. Tuck, “A version of the aitken accelerator for computer iteration,” *International Journal for Numerical Methods in Engineering*, vol. 1, no. 3, pp. 275–277, 1969.
- [32] B. W. Uekermann, “Partitioned fluid-structure interaction on massively parallel systems,” Ph.D. dissertation, Technische Universität München, 2016.

- 
- [33] R. Haelterman, J. Degroote, D. Van Heule, and J. Vierendeels, “The quasi-newton least squares method: a new and fast secant method analyzed for linear systems,” *SIAM Journal on numerical analysis*, vol. 47, no. 3, pp. 2347–2368, 2009.
- [34] B. Uekermann, H.-J. Bungartz, B. Gatzhammer, and M. Mehl, “A parallel, black-box coupling algorithm for fluid-structure interaction,” in *Proceedings of 5th International Conference on Computational Methods for Coupled Problems in Science and Engineering*, 2013, pp. 1–12.
- [35] R. Haelterman, A. E. Bogaers, K. Scheufele, B. Uekermann, and M. Mehl, “Improving the performance of the partitioned qn-ils procedure for fluid–structure interaction problems: Filtering,” *Computers & Structures*, vol. 171, pp. 9–17, 2016.
- [36] D. Blom, F. Lindner, M. Mehl, K. Scheufele, B. Uekermann, and A. van Zuijlen, “A review on fast quasi-newton and accelerated fixed-point iterations for partitioned fluid–structure interaction simulation,” in *Advances in Computational Fluid-Structure Interaction and Flow Simulation*. Springer, 2016, pp. 257–269.
- [37] F. Lindner, M. Mehl, K. Scheufele, and B. Uekermann, “A comparison of various quasi-newton schemes for partitioned fluid-structure interaction,” in *Proceedings of 6th International Conference on Computational Methods for Coupled Problems in Science and Engineering, Venice*, 2015, pp. 1–12.
- [38] T. Kajishima and K. Taira, “Immersed boundary methods,” in *Computational Fluid Dynamics*. Springer, 2017, pp. 179–205.
- [39] R. van Loon, P. D. Anderson, F. N. van de Vosse, and S. J. Sherwin, “Comparison of various fluid–structure interaction methods for deformable bodies,” *Computers & structures*, vol. 85, no. 11-14, pp. 833–843, 2007.
- [40] C. Degand and C. Farhat, “A three-dimensional torsional spring analogy method for unstructured dynamic meshes,” *Computers & structures*, vol. 80, no. 3-4, pp. 305–316, 2002.
- [41] A. O. González, A. Vallier, and H. Nilsson, “Mesh motion alternatives in openfoam,” *PhD course in CFD with OpenSource software*, 2009.
- [42] H.-J. Bungartz, F. Lindner, B. Gatzhammer, M. Mehl, K. Scheufele, A. Shukaev, and B. Uekermann, “precice—a fully parallel library for multi-physics surface coupling,” *Computers & Fluids*, vol. 141, pp. 250–258, 2016.
- [43] F. Lindner, M. Mehl, and B. Uekermann, “Radial basis function interpolation for black-box multi-physics simulations,” 2017.
- [44] S. Chen, M. t. Wambsganss, and J. Jendrzejczyk, “Added mass and damping of a vibrating rod in confined viscous fluids,” in *asme*, 1976.
- [45] C. Conca, A. Osses, and J. Planchard, “Added mass and damping in fluid-structure interaction,” *Computer methods in applied mechanics and engineering*, vol. 146, no. 3-4, pp. 387–405, 1997.
- [46] J. Gauthier, A. Giroux, S. Etienne, and F. Gosselin, “A numerical method for the determination of flow-induced damping in hydroelectric turbines,” *Journal of Fluids and Structures*, vol. 69, pp. 341–354, 2017.

- [47] G. Ricciardi and E. Boccaccio, “Modelling of the flow induced stiffness of a pwr fuel assembly,” *Nuclear Engineering and Design*, vol. 282, pp. 8–14, 2015.
- [48] P. Causin, J.-F. Gerbeau, and F. Nobile, “Added-mass effect in the design of partitioned algorithms for fluid–structure problems,” *Computer methods in applied mechanics and engineering*, vol. 194, no. 42-44, pp. 4506–4527, 2005.
- [49] J. Degroote, P. Bruggeman, R. Haelterman, and J. Vierendeels, “Stability of a coupling technique for partitioned solvers in fsi applications,” *Computers & Structures*, vol. 86, no. 23-24, pp. 2224–2234, 2008.
- [50] T. Bodnár, G. P. Galdi, and Š. Nečasová, *Fluid-structure interaction and biomedical applications*. Springer, 2014, ch. 13.
- [51] C. Förster, W. A. Wall, and E. Ramm, “The artificial added mass effect in sequential staggered fluid-structure interaction algorithms,” in *ECCOMAS CFD 2006: Proceedings of the European Conference on Computational Fluid Dynamics, Egmond aan Zee, The Netherlands, September 5-8, 2006*. Delft University of Technology; European Community on Computational Methods . . . , 2006.
- [52] B. Gatzhammer, “Efficient and flexible partitioned simulation of fluid-structure interactions,” Ph.D. dissertation, Technische Universität München, 2014.
- [53] B. Uekermann, H.-J. Bungartz, L. Cheung Yau, G. Chourdakis, and A. Rusch, “Official precice adapters for standard open-source solvers,” in *Proceedings of the 7th GACM Colloquium on Computational Mechanics for Young Scientists from Academia*, 2017.